Study of the Effect of Fracture Completion Variables on Decline Curve Parameters for Long-Term Production Forecast of Shale Liquids

A Thesis

Presented to

The Faculty of the Department of Chemical Engineering

University of Houston

In Partial Fulfillment

Of the Requirements for the Degree of

Master of Science

In Petroleum Engineering

by

Eshwar C Yennigalla

December 2013

Study of the Effect of Fracture Completion Variables on Decline Curve Parameters for Long-term Production Forecast of Shale Liquids

---

Eshwar C. Yennigalla

Approved:

Chair of the Committee
Dr. W. John Lee,
Hugh Roy and Lillie Cranz
Cullen Distinguished University
Chair Professor,
Petroleum Engineering

Committee Members:

Dr. Thomas Holley,
Professor and Director,
Petroleum Engineering

Dr. Michael Myers,
Professor,
Petroleum Engineering

Dr. Guan Qin,
Professor,
Petroleum Engineering

Dr. Suresh Khator,
Associate Dean
Cullen College of Engineering

Dr. Michael Harold,
Department Chair,
Chemical Engineering

ACKNOWLEDGEMENTS

I would like to dedicate this work to my beloved family for their constant encouragement, support and unconditional love. I am deeply indebted to them.

I am grateful to my advisor, Dr. John Lee for giving me an opportunity to pursue a Master's thesis under his esteemed guidance. His constant presence, encouragement and vision have helped me develop as a graduate student and as a person. I would like to thank him for providing me the opportunity to be a part of his graduate student research team.

My special thanks to Dr. Thomas Holley, Dr. Michael Myers, and Dr. Guan Qin for accepting the invitation to serve on my thesis committee. I would like to extend my deepest gratitude for your invaluable suggestions and support. A special mention of gratitude to Ms. Anne Sturm. If it was not for your constant effort it be would be impossible for me to achieve my goals.

Study of the Effect of Fracture Completion Variables on Decline Curve Parameters for Long-term Production Forecast of Shale Liquids

An Abstract

Of a Thesis

Presented to

The Faculty of the Department of Chemical Engineering

University of Houston

In Partial Fulfillment

Of the Requirements for the Degree of

Master of Science

In Petroleum Engineering

by

Eshwar C Yennigalla

December 2013

Abstract

Shale reservoir exploitation using multiple stage hydraulically fractured horizontal wells has proved the existence of considerable amount of oil and gas reserves throughout the world. Forecasts of future production from these reservoirs based on the fracture stimulation parameters and reservoir properties has led to a better understanding of the duration of important flow regimes and parameters used in production forecasting models. The decline curve analysis considered in the study is a combination of the traditional Arps and Stretched Exponential production decline models designed to fit the forecasts for individual flow regime production data.

Simulations using identical reservoir properties but different fracture completion parameters were analyzed and fit to decline models. The parameters considered in our study are fracture half-length, fracture spacing, stimulated reservoir volume permeability and matrix permeability.

TABLE OF CONTENTS

LIST OF FIGURES

LIST OF TABLES

NOMENCLATURE

b	=	Arps decline exponent
D_i	=	Arps Decline rate (T^{-1})
q_t	=	Oil Production Rate (L^3T^{-1})
$N_{p(t)}$	=	Cumulative Oil Production (L^3)
t	=	Production Time (T)
r_e	=	Effective Reservoir Radius (L)
r_w	=	Wellbore Radius (L)
q_D	=	Dimensionless Rate
t_D	=	Dimensionless Time
q_{dD}	=	Fetkovich Dimensionless Rate
t_{dD}	=	Fetkovich Dimensionless Time
τ	=	Time component in Stretched Exponential Production Decline (T)
η	=	Exponent in Stretched Exponential Production Decline
t_{bdf}	=	Time to boundary dominated flow
ϕ	=	Reservoir Porosity
μ	=	Reservoir fluid viscosity ($FL^{-2}T$)
c_t	=	Total compressibility (L^2F^{-1})
k	=	Zone Permeability (L^2)

ABBREVATIONS

EIA = Energy information administration

SRV = Stimulated reservoir volume

BDF = Boundary dominated flow

MBT = Material balance time

EUR = Estimated Ultimate Recovery

Chapter 1

Introduction

1.1 Overview

This thesis is composed of studies related to three topics: (1) Sensitivity analysis of fracture completion variables in production profiles; (2) analysis of the variation of decline curve parameters in boundary dominated flow regimes and (3) comparison of depth of investigation estimated from theoretical equations with estimates from diagnostic plots to yield the time to start to boundary dominated flow. Our plan is to describe the status of shale oil production in the United States, stimulation techniques used to produce hydrocarbons at economically viable rates, decline curve analysis techniques and depth of investigation equations in Chapter 1 and then discuss simulation input variables and the results of our analysis in later chapters.

1.2 Unconventional resources

Unconventional or non-traditional reservoirs are defined as the reservoirs that cannot be produced at economic flow rates without large external stimulation techniques or other special recovery technologies. Unconventional resources (UCR) consist of oil and gas extracted from shales

and coal, bitumen from oil sands and gas from hydrates. UCR yield the same type of final product as that of conventional resources, regardless of the extraction technology.

The resource triangle approach helps us understand that oil and gas resources, especially UCR are extensive. Markets always balance global supply and demand; however, UCR need higher pricing and new technologies. Figure 1 illustrates that conventional resources represent a relatively small volume of the total reserves but are less expensive to produce. Unconventional resources depicted by the lower part of the triangle tend to occur in substantially higher volumes but require expensive technologies and higher prices to be economically viable.

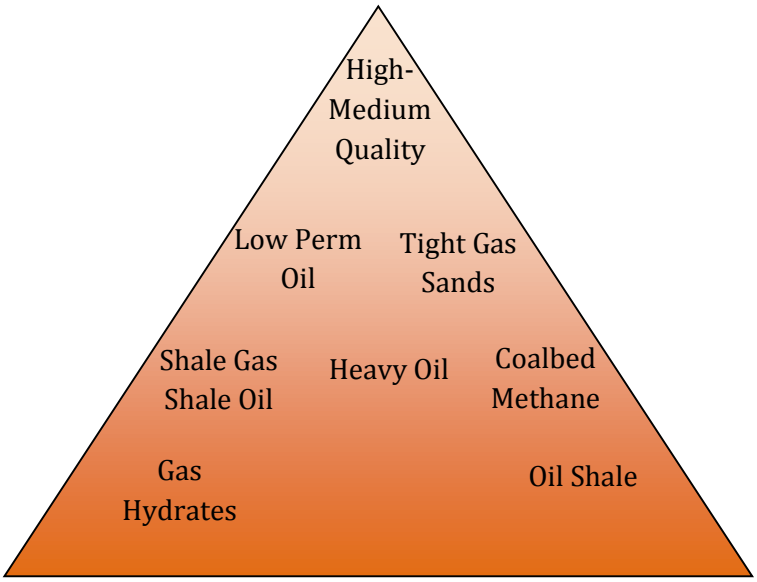

Figure 1. The resource triangle.

Shale plays have led to the second biggest oil boom in history. Shale oil and gas production in North America have seen a tremendous rise due to the advent of multiple stage long hydraulic fractures in the last decade. Figure 2 shows the US Energy Information Administration (EIA) estimates for crude oil production in the US in the current century. The steep increase in production from the mid-2000's is mainly due to production from shale oil reserves. It is estimated that shale oil production might become larger than traditional oil production after the mid-2020's. There has been a 13% increase in oil production in US in the last 10 years. According to the US energy consultancy PIRA, the United States has overtaken Saudi Arabia and Russia to become the world's biggest oil producer.

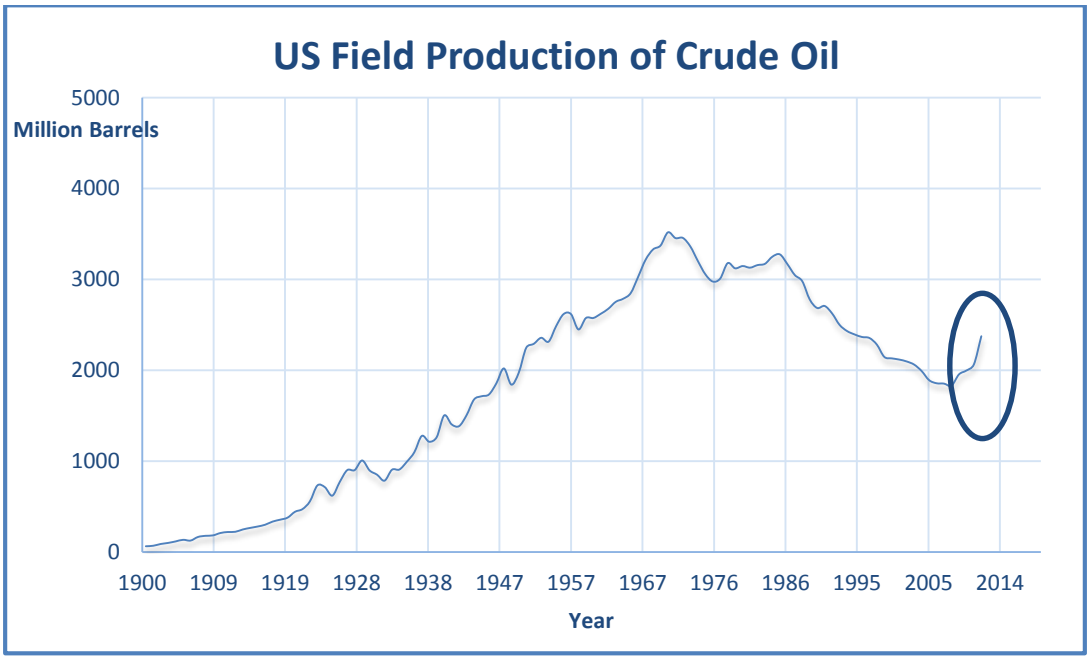

Figure 2. US field production of crude oil.

Figure 3 shows the EIA estimates for dry natural gas production in the US; and it indicates that production has increased exponentially in the past decade. There has been a 27% increase in oil production in US in the last 10 years. As a result, the United States is set to overtake Russia as the leading natural gas producer in the world.

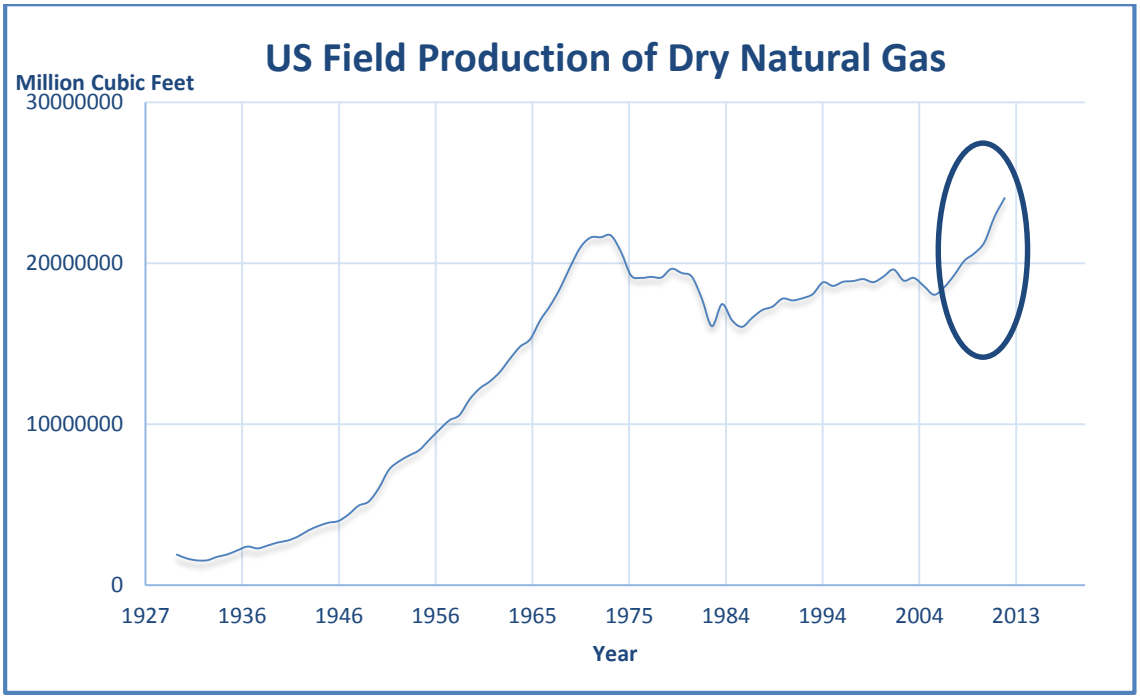

Figure 3. US field production of dry natural gas.

The impact created by the advent of production from shale reservoirs using multiple stage hydraulic fracturing has changed the perception of oil and gas industry globally and provided economic boost around the newly found basins in US. However, the higher production is accompanied by higher initial costs for stimulation techniques. Investment decisions depend

on forecasts of oil and gas production in these horizontal wells which, in turn, depend on the fracture completion parameters of these wells. Our study involves examining the effect of these completion parameters on the parameters in the production decline models.

1.3 Production techniques in shale plays

Figure 4 depicts the distribution of shale plays in United States (EIA 2011). Characterizing these shale plays can be challenging as the rock properties vary significantly from one shale play to another. Formations in each shale play are found to be unique; also their mechanical anisotropy is different due to organized distribution of clay minerals. The common unifying factors in all the shale plays are the low reservoir/matrix permeabilities of the order of $1x\ 10^{-4}$ md and porosities between 3 to 6 percent. Due to such low permeability, recovery factors from traditional vertical wells are not economic and wells require special stimulation techniques.

Horizontal wells with multiple hydraulic fractures penetrating deep laterally into the reservoir would provide a much higher effective permeability in the region affected by fractures. The region penetrated by the hydraulic fractures is called the Stimulated Reservoir Volume (SRV),

and with the effective permeability in the matrix appears to be one or two orders higher than the unstimulated matrix permeability, perhaps due to reopening of closed natural fractures and creation of new micro-fractures. This SRV effective permeability does not include the permeability of the hydraulic fractures. Figure 5 depicts a typical multi-fractured horizontal well.

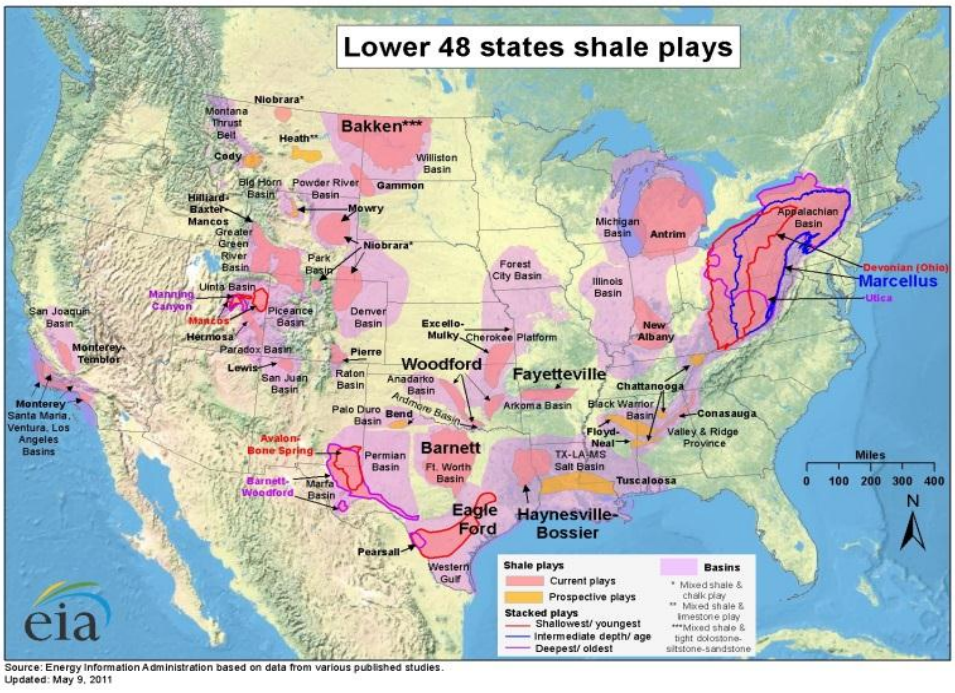

Figure 4. Distribution of Shale Plays in United States (EIA 2011).

A large volume of water with proppant (e.g., sand) is pumped into the reservoir at high rates and pressure, breaking and opening the reservoir rock then extending the fractures deep into the reservoir. This creates conduits of high conductivity and variable size to produce oil and gas.

Study of the effects of these multiple hydraulic fractures on long term production is essential in designing, planning and constructing the horizontal well, completing the well and fracturing the reservoir.

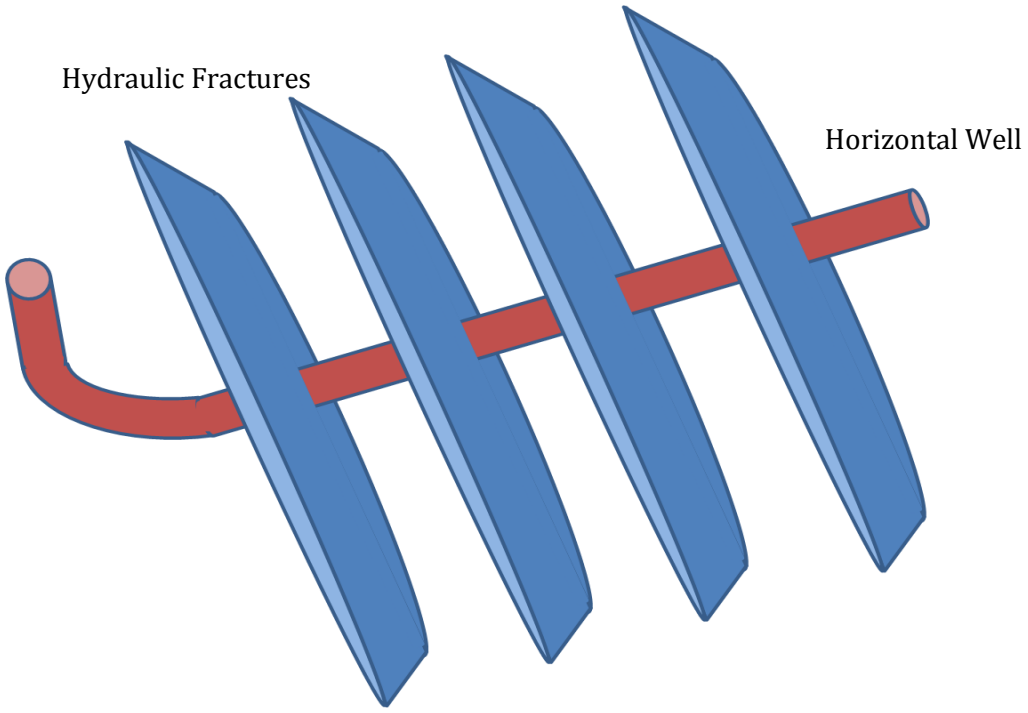

Figure 5. A typical multi-stage hydraulic fracture.

1.4 Decline Curve Analysis

Decline curve analysis has been among the most common and accepted methods to forecast production and estimate reserves in traditional resource plays. Decline curves extrapolate the historical production data into the future by means of algorithms constructed using observed rate of decline in production. The forecast generated by the decline curve is used to make the

key investment decisions in current wells and for wells considered to be analogues to the current well.

Traditional decline curves fail, however, to generate accurate production forecasts in shale plays due to difference in lengths of flow regimes. In shale reservoir production, transient flow can extend up to 15-20 years until interference between adjacent hydraulic fractures is observed. After transient flow ends with fracture interference, the boundary-dominated flow (BDF) regime prevails. Decline methods involving initial transient flow followed by BDF are useful in these cases, and have been included in this study.

1.5 Depth of Investigation Equations

Depths of investigation calculations are helpful to describe durations of flow regimes in both conventional and unconventional reservoirs. By characterizing flow regimes for multistage hydraulic fracture systems, we can optimize the fracture stages. Lee (1982) introduced the concept of radius of investigation and Kang et al. (2011) provides depth of investigation equations to find the time to BDF. The application of these equations along with the study of behavior of the BDF regime should lead to better long-term production forecasts in the industry.

1.6 Objective of the study

The objective of this study is to determine parameters in production decline models useful in ultra-low permeability reservoirs producing from horizontal wells with multi-stage hydraulic fractures.

Chapter 2

Decline Curve Analysis

The term "Decline Curve Analysis" (DCA) is used in the petroleum industry to describe graphical projection of the flow rate decline trend of a well into the future and from that projection, estimation of the remaining well life (Hughes, 1967). This is the most common means of forecasting production and estimating the value of oil and gas wells. Traditional decline curve analysis considers particular cases of production decline in wells producing with constant bottom-hole pressure which implies continuous drop of production rate with time.

The major assumptions in most common DCA model Arps are: (1) Constant BHP production, (2) Boundary-dominated flow; and (3) constant productivity index. Decline curve analysis is normally done by extrapolation of a performance trend using a certain function based on the type of reservoir. The function considered has to be a continuous function of the independent variable, time. The extrapolation to a specified endpoint should yield an estimate of the ultimate recovery.

Other decline models have been introduced in recent years and include; Stretched Exponential Production Decline (SEPD), Power Law Production

Decline and Duong Production Decline models, all of which are primarily for transient flow. In our study we have considered a combination of Arps and SEPD models.

2.1 Arps Decline Model

Arps, J J reported this decline model in 1945; it is often considered to be the beginning of modern decline curve analysis. The work led to formulation of three variations of the model: exponential, hyperbolic and harmonic rate decline relations. The simplicity and consistency of this approach led it to become the benchmark for analysis and interpretation of production data in the industry.

The Arps rate relations are

Case	Relation	
Exponential Decline ($b = 0$)	$q_t = q_i \exp(-D_i t)$,	(2.1)
Hyperbolic Decline ($0 < b < 1$)	$q_t = \frac{q_i}{(1+bD_i t)^{\frac{1}{b}}}$, and	(2.2)
Harmonic Decline ($b = 1$)	$q_t = \frac{q_i}{(1+bt)}$.	(2.3)

The Arps cumulative production relations are:

Case	Relation	
Exponential Decline ($b = 0$)	$N_p(t) = \frac{q_i}{D_i}[1 - \exp(-D_i t)]$,	(2.4)

Hyperbolic Decline ($0 < b < 1$) $N_p(t) = \frac{q_i}{(1-b)D_i}\left[1 - (1 + bD_i t)^{1-1/b}\right]$, and (2.5)

Harmonic Decline ($b = 1$) $N_p(t) = \frac{q_i}{D_i}\ln(1 + D_i t).$ (2.6)

These relations accurately predict the production decline in traditional or conventional resource plays since the flow is primarily BDF which occurs after the radius of drainage has reached the outer boundaries and the well is draining a constant reservoir volume. The relations limit b to a value equal or less than 1 which is appropriate for analysis of BDF declines. However, in multi-stage hydraulic fractured reservoirs, long-duration transient flow behavior results in apparent values of b higher than 1 (even up to 2.5 or more) which alters forecasted decline patterns of production rates. The Arps equations may fail to provide accurate forecasts of shale oil produced from hydraulic fractures.

2.2 Fetkovich Type Curves

Fetkovich (1980) introduced type-curve matching of production data for a well, produced at a constant bottom-hole pressure. Fetkovich generated type curves for the transient flow decline using analytical solutions for radial drainage systems and combined them with the boundary dominated flow decline type curves based on the Arps equations.

Figure 6 illustrates Fetkovich type-curve, the vertical axis represents dimensionless decline rate, q_{dD} and the horizontal axis represents dimensionless decline time, t_{dD}.

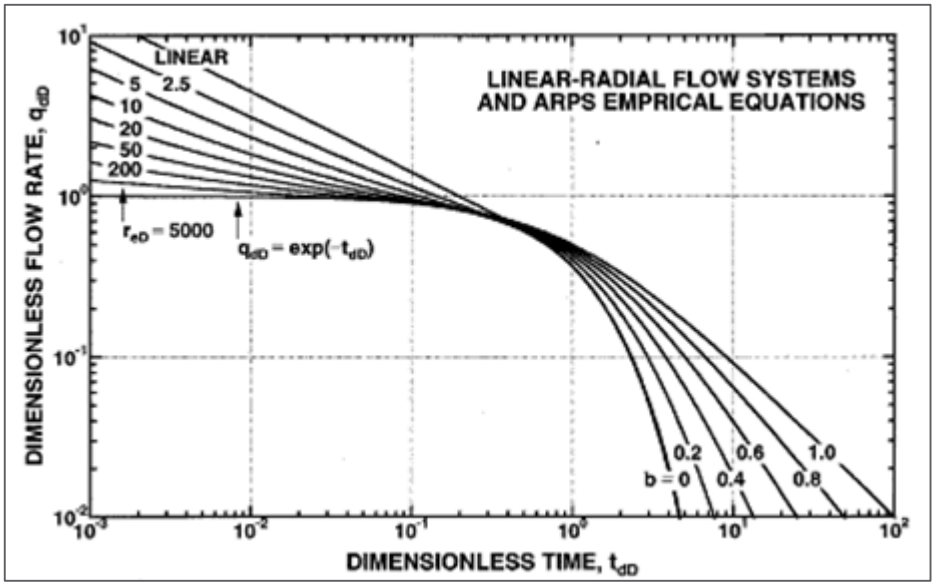

Figure 6 Log-log plot of q_{dD} vs. t_{dD} (best interpreted as $q/(p_i - p_{wf})$ vs. t for field data) indicating the characteristic influence of boundary-dominated flow [Chen and Teufel (2000)].

All curves on the right are concave downward, whereas data in transient flow (on the left) will be concave upward (radial flow) or straight (linear or bilinear flow). The transient linear flow regime is characterized by an Arps decline constant, b, of 2.0. Bilinear flow would fall on a straight line with b = 4.0. The early time curves are based on analytical solutions to flow equations for transient radial and linear flow, stated in terms of Fetkovich's definitions of dimensionless rates and times:

$$q_{dD} = q_D \left[\ln\left(\frac{r_e}{r_w}\right) - \frac{1}{2}\right] \text{ and} \tag{2.7}$$

$$t_{dD} = \frac{t_D}{\frac{1}{2}\left[\left(\frac{r_e}{r_w}\right)^2 - 1\right]\left[\ln\left(\frac{r_e}{r_w}\right) - \frac{1}{2}\right]}, \tag{2.8}$$

where,

$$q_D = \frac{141.2\, B\mu}{kh(p_i - p_{wf})}\ and$$

$$t_D = \frac{0.00633k}{\emptyset \mu c_t r_{wa}^2} t.$$

The late time behavior curves are based on Arps' decline models and Fetkovich's definitions of dimensionless rates and times in terms of Arps parameter can be expressed as

$$q_{DdD} = \frac{q(t)}{q_i}, \text{ and} \tag{2.9}$$

$$t_{DdD} = D_i t\ , \tag{2.10}$$

where,

$$q_t = \frac{q_i}{(1 + bD_i t)^{\frac{1}{b}}}.$$

The relation between q_t and t is the Arps hyperbolic decline equation.

2.3 Stretched Exponential Production Decline Analysis

Valko (Valko, 2009) proposed Stretched Exponential Production Decline analysis to account for transient production decline, common in low permeability reservoirs for long times (months or years). The model states

that the actual production decline is determined by exponential decay of reservoir fluid rates with a continuous distribution of decay parameters, τ.

The SEPD relations are

Case	Relation	
Production Rate	$q_t = q_i \exp\left(-\left(\frac{t}{\tau}\right)^{\eta}\right)$ and	(2.11)
Cumulative Production	$N_p = \frac{q_i \tau}{\eta}\left\{\Gamma\left(\frac{1}{\eta}\right) - \Gamma\left(\frac{1}{\eta}, \left(\frac{t}{\tau}\right)^{\eta}\right)\right\}$.	(2.12)

The distribution is governed by (η, τ) (Valko and Lee, 2010).The parameter η plays the role of b in the Arps equations. The determination of these parameters involves solving two nonlinear equations. The ratios of second year cumulative flow to the first year cumulative flow and the third year cumulative flow to the first year cumulative flow are used in the calculations.

$$r_{21} = \frac{N_{p,second\ year}}{N_{p,first\ year}} \text{ and} \tag{2.13}$$

$$r_{31} = \frac{N_{p,third\ year}}{N_{p,first\ year}}. \tag{2.14}$$

Using the cumulative production relations the above relations can be represented by

$$\frac{\Gamma\left(\frac{1}{\eta}\right) - \Gamma\left(\frac{1}{\eta}, \left(\frac{24}{\tau}\right)^{\eta}\right)}{\Gamma\left(\frac{1}{\eta}\right) - \Gamma\left(\frac{1}{\eta}, \left(\frac{12}{\tau}\right)^{\eta}\right)} = r_{21} \text{ and} \tag{2.13}$$

$$\frac{\Gamma\left(\frac{1}{\eta}\right)-\Gamma\left(\frac{1}{\eta},\left(\frac{36}{\tau}\right)^{\eta}\right)}{\Gamma\left(\frac{1}{\eta}\right)-\Gamma\left(\frac{1}{\eta},\left(\frac{12}{\tau}\right)^{\eta}\right)}=r_{31}. \quad (2.14)$$

In contrast to Arps, SEPD predicts realistic results for unconventional (tight) reservoirs since the exponential decay leads to steep production declines and also closely follows analytical solutions for lower permeability and longer transition flows. Also the EUR forecasted using b values higher than 1 can be infinitely large whereas the late time behavior of SEPD is comparable to observed behavior in unconventional reservoirs and EUR is bounded.

2.4 Composite Model

The need to develop more accurate production decline models satisfying analytical solutions and providing accurate results led us to take Fetkovich's approach of different systems for transient and boundary dominated flow regimes. We used SEPD for the transient flow regime and Arps equations for the BDF regimes. The switch between the SEPD and Arps model is made at the onset of BDF which is identified using either depth of investigation calculations or various diagnostic plots discussed in the next chapter.

The issue here is to generate a continuous decline curve unlike the case of Fetkovich type curves. To maintain the continuity the rates and the slopes of the curves need to be same at the switch, t_{sw}. The rate, q_{sw}, at the end of

transient flow becomes q_i in the Arps hyperbolic model; the decline rate, D_{sw}, at the end of transient flow becomes D_i in the Arps decline model, and elapsed time in the Arps model becomes (t - t_{sw}). In this way, the value and the slope of the rate-time curve is preserved (Nobakht, et al., 2010). The b value is generated by finding a best-fit to rate-time data on the Fetkovich type curves.

Chapter 3

Depth of Investigation Equations and Techniques

Multi-stage hydraulic fractures in shale reservoirs exhibit long transient flow. There are many techniques available in the industry to identify the flow regime and generate the time at which the shift occurs from linear flow to boundary dominated flow. These techniques can be classified as "pressure transient analysis" and "rate transient analysis." In this chapter we discuss rate transient analysis techniques and the depth of investigation equations used in our study.

3.1 Depth of Investigation Equations

Depth of investigation equations give the distance away from a well or hydraulic fracture at which the presence of the fracture is felt; i.e., at that particular instant the reservoir fluid at that distance first starts to move towards the well or fracture. These equations have been derived for various scenarios such as a vertical well with radial flow towards the well and a horizontal well with fractures. The modelling equation for each scenario is different. The objective in our study is to identify the time of onset of boundary dominated flow either by reaching the unstimulated reservoir

area or by interference from adjacent fractures. The time to boundary dominated flow (Kang, et al., 2011) is given by

$$t_{bdf} = \frac{1896(\emptyset \mu c_t)_i d_b^2}{k}. \quad (3.1)$$

The time to boundary dominated flow is dependent on both the reservoir properties and fracture completion properties. The distance used in the equation can be the fracture spacing or the distance from the well to its drainage boundary depending on which boundary is first considered to be encountered. We believe that fracture interference will occur before flow from the unstimulated region commences.

3.2 Material Balance Time Diagnostic Plot

A log-log plot of rate vs. material balance time provides the potentially most reliable insight into flow regimes encountered during production history. Material balance time is calculated using cumulative production and the production rates given by

$$MBT = \frac{Cumulative\ Production}{Production\ Rate}. \quad (3.2)$$

As shown in Figure 7 the flow regimes are represented by straight lines in the log-log plots. Half slope line represents the linear flow regime, quarter slope line represents bilinear flow regime and the unit slope line represents boundary dominated flow. In multi-stage fractures there is a

chance to have bilinear flow initially for a short period of time followed by a long linear flow and maybe end with boundary dominated flows.

The time to boundary dominated flow is calculated when the slope of the production profile switches to unit slope. The time calculation however is based on individual perception of identification of unit slope and the results may vary by several months from person to person. We calculated the time to BDF by calculating and analyzing the log slope of the material balance time plot. In most cases the time to BDF was calculated when the slope approached a value of -0.9 and in cases where a value of -0.9 was not reached, the point where the slope approached -0.85 was selected as the time to BDF.

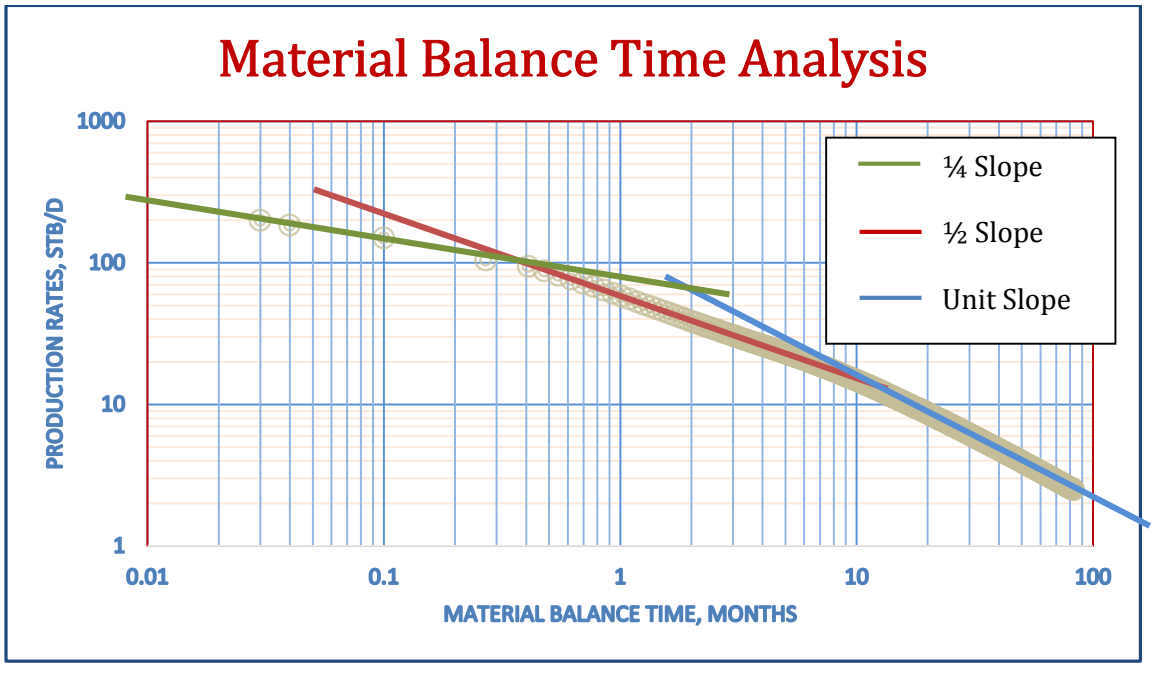

Figure 7. Material balance time analysis.

3.3 Square-Root-of-Time Diagnostic Plot

A plot of rate-normalized pressure vs. square-root of time also enables us to study the flow regimes based on production history. As shown in Figure 8 the initial straight line represents linear flow and the later straight line represents the BDF. The time to BDF can be calculated at the deviation from the initial straight line.

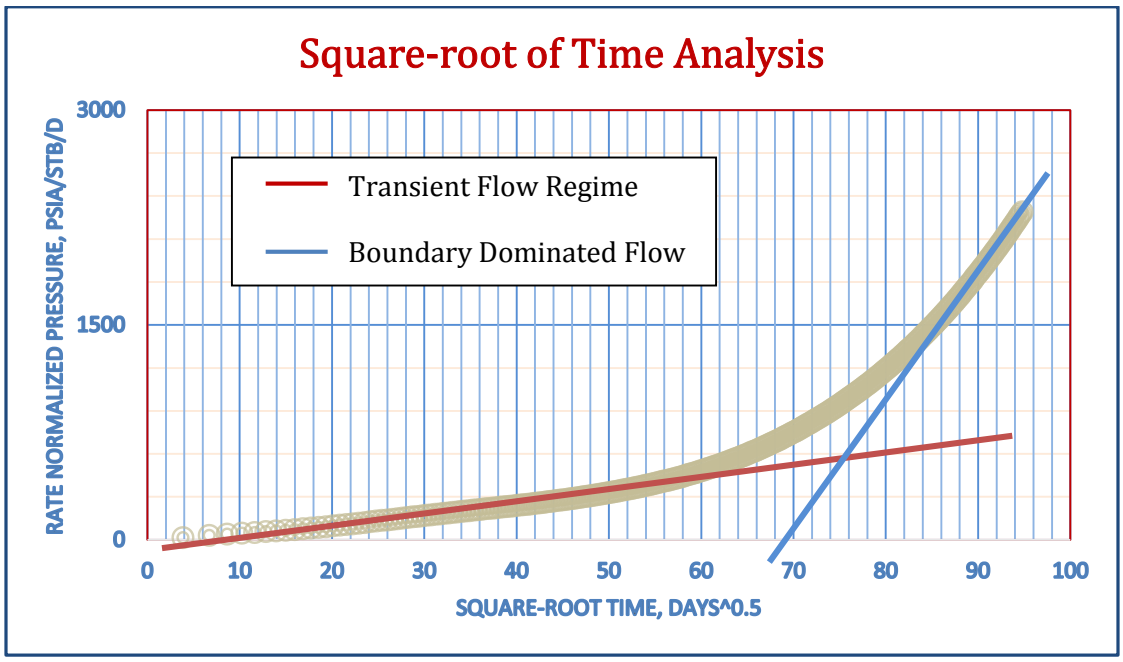

Figure 8 Square-root of time analysis.

Chapter 4

Numerical Simulation

Reservoir, reservoir fluid and completion parameters consistent with the Bakken field were used in the numerical simulation model of this study. The model input parameters and simulation cases are described in this chapter.

4.1 Bakken Formation

Bakken shale is the one of the largest oil reservoirs in the United States. It is estimated to have 200 billion barrels of oil in place (Flannery 2006). It stretches across North Dakota, South Dakota and Montana. The Bakken shale play was discovered in 1980 but development has been slow and was mostly ignored due to the low permeability of the reservoir. The formation is mostly over pressured, and over-pressuring may have led to the creation of natural fractures within the formation. Figure 9 shows the distribution of Oil and Natural Gas wells in the Bakken formation, western part of North Dakota (DrillingInfo, 2013).

The formation thickness ranges from 0-140 ft with the central section being the thickest. The upper and lower members act as source rock and have permeabilities ranging from 10-100 nano Darcies (Tran 2011). The reservoir fluid is categorized as light oil (42^0 API) and sweet oil due to

absence of H_2S (Philips 2007). The viscosity is about 0.36 cp. The initial water saturation varies from 30 to 60% (Cox 2008).

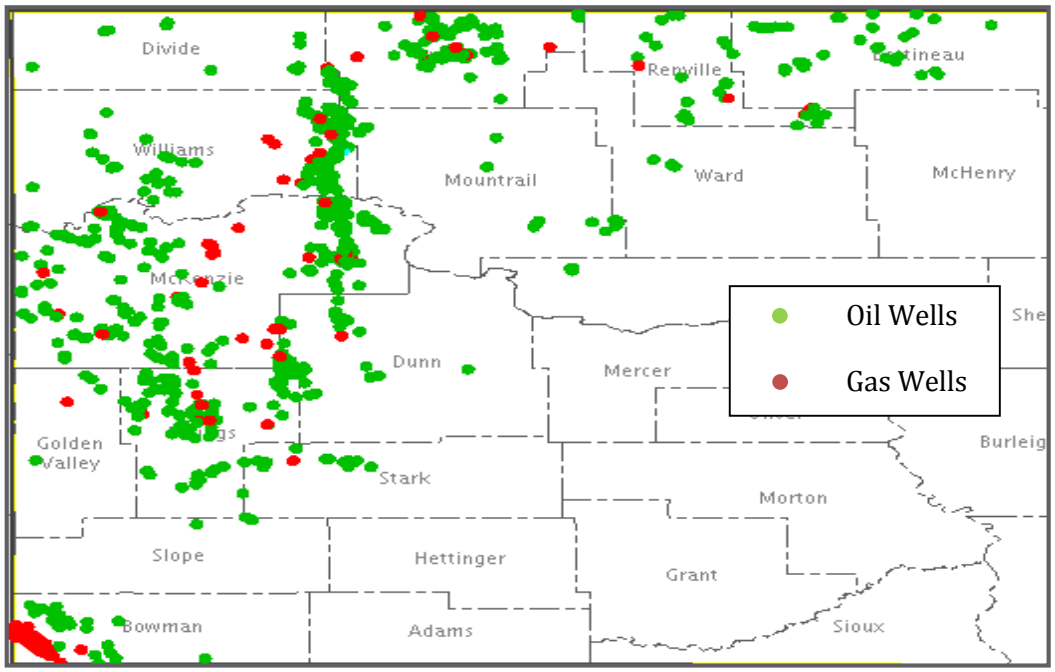

Figure 9. Distribution of oil and natural gas wells in the Bakken formation, western part of North Dakota, DrillingInfo, 2013.

4.2 Reservoir Model

As discussed in the previous chapter unconventional shale oil and gas reservoirs require multi-stage fractures in a horizontal well. Figure 10 is schematic of a typical well in a shale reservoir. The white colored region is the Stimulated Reservoir Volume (SRV), the green zone is the unstimulated reservoir and the yellow planes are the hydraulic fractures. Reservoir Properties, PVT properties and completions parameters used for the mother simulation are presented in Table 1, Table 2 and Table 3 respectively.

The Fekete Harmony composite based numerical model was used. The underlying assumption of the analytical models for production data analysis is single-phase flow in the reservoir (Fekete Harmony 2013 v2). In order to accommodate multiple flowing phases, the model must be able to handle changing fluid saturations and relative permeabilities. Since these phenomena are highly non-linear, analytical solutions are very difficult to obtain and use. Thus, numerical models are generally used to provide solutions for the multiphase flow problem. The numerical engine used in the software is based on a general purpose black-oil simulator. Numerical models can be created with less simplifying assumptions for reservoir properties than analytical models. The reservoir heterogeneity, mass transfer between phases, and the flow mechanisms can be incorporated rigorously.

Numerical models solve the nonlinear partial-differential equations (PDE's) describing fluid flow through porous media with numerical methods. Numerical methods are the process of discretizing the PDE's into algebraic equations and solving those algebraic equations to obtain the solutions. These solutions that represent the reservoir behavior are the values of pressure and phase saturation at discrete points in the reservoir and at discrete times.

The advantage of the numerical method approach is that the reservoir heterogeneity, mass transfer between phases, and forces/mechanisms responsible for flow can be taken into consideration adequately. For instance, multiphase flow, capillary and gravity forces, spatial variations of rock properties, fluid properties, and relative permeability characteristics can be represented accurately in a numerical model.

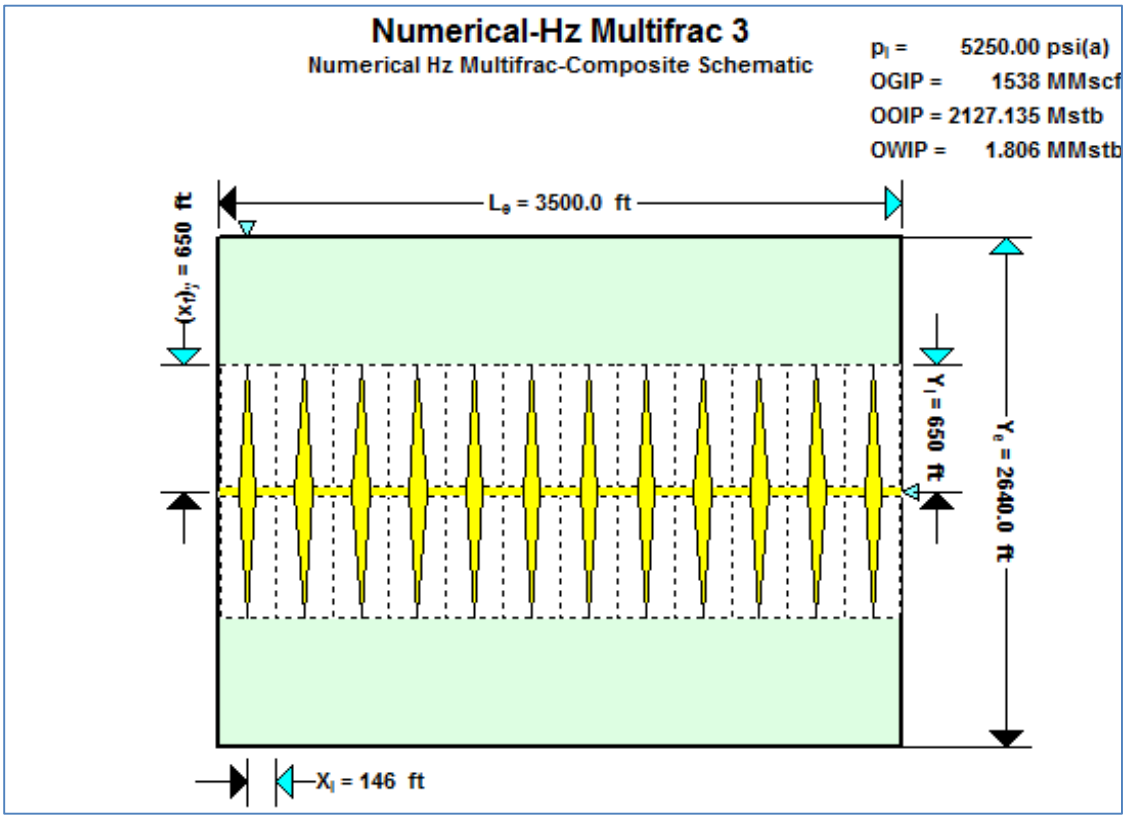

Figure 10. Numerical simulation schematic of SRV and unstimulated regions.

In general, analytical methods provide exact solutions to simplified problems, while numerical methods yield approximate solutions to the exact problems. One consequence of this is that the level of detail and time required

to define a numerical model is more than its equivalent analytical model. The composite analytical model allows one to investigate the extent of the contribution from the unstimulated matrix region (Thompson 2011).

Table 1. Reservoir properties for base simulation.

Property	Value
Reservoir pressure	5250 psi
Reservoir temperature	245^0F
Thickness	50 ft
Porosity	6%
SRV permeability	0.001 md
Matrix permeability	0.0001 md
Total compressibility	$1.45*10^{-5}$ $psia^{-1}$

Table 2. PVT properties for base simulation.

Property	Value
Oil saturation	62%
Oil viscosity	0.36 cp
^{0}API	42^0
Oil density	39.8 lb/ft^3
Oil compressibility	$1.17*10^{-5}$ $psia^{-1}$

Table 3. Completion parameter for base simulation

Property	Value
Horizontal well length	3500 ft
Fracture half-length	650 ft
Reservoir width	2640 ft
Dimensionless fracture conductivity	300
Number of fractures	25
Fracture spacing	140 ft
Wellbore radius	0.35

4.3 Simulation Results

The above model was used to simulate a typical Bakken well using Fekete Harmony (v2 2013); Figure 8 shows the pressure variation in the reservoir at 300 months. The well was produced with a bottom-hole pressure of 1000 psi. Figures 11, 12, 13, 14, 15 and 16 show the pressure distribution in the reservoir through the production life of the well. The initial flow is perpendicular to the fracture orientation and the flow inside the fracture contributes to bilinear flow regime conditions in many situations. This regime usually has a very short life span.

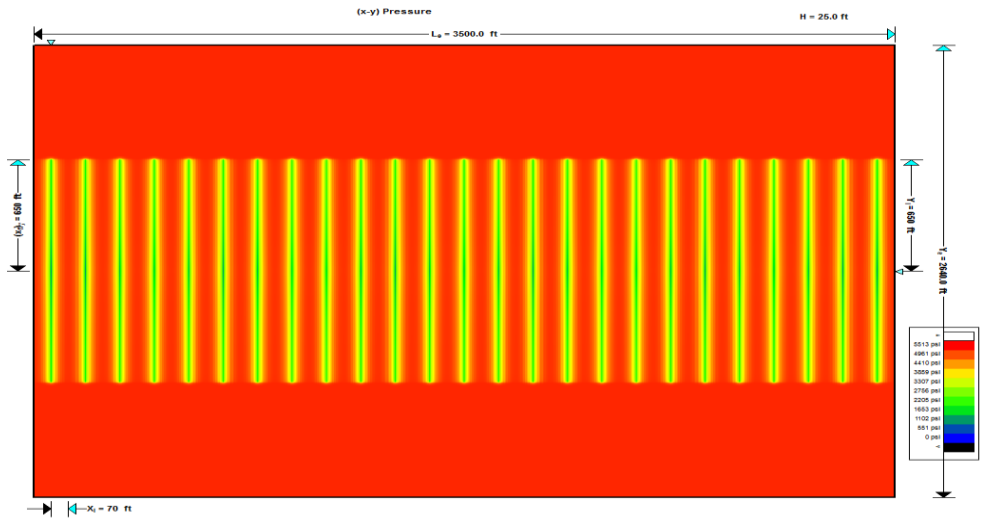

Figure 11. Pressure distribution in the reservoir after 3 months of production

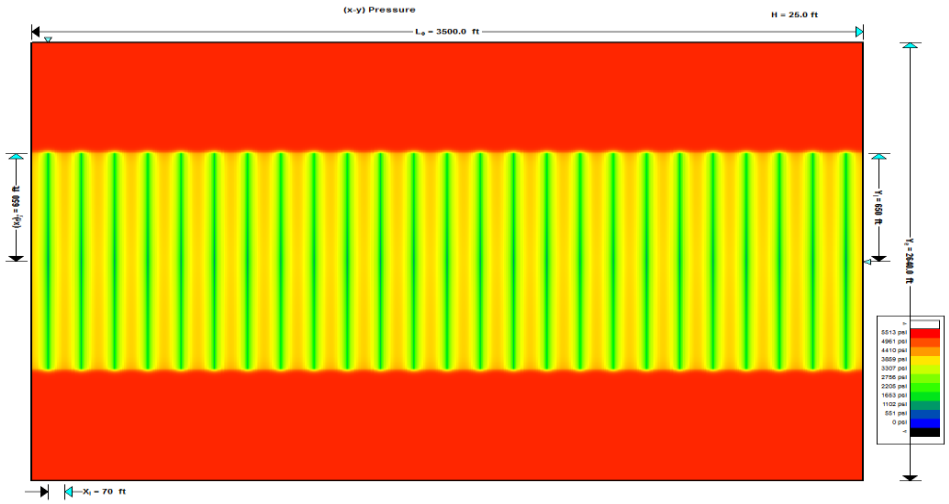

Figure 12. Pressure distribution in the reservoir after 6 months of production

The initial pressure distribution after 3 months of production shows that production occurs essentially along the fracture alone. After 6 months of production pressure decline begins to spread throughout the SRV. The pressure distribution throughout the SRV is still not uniform.

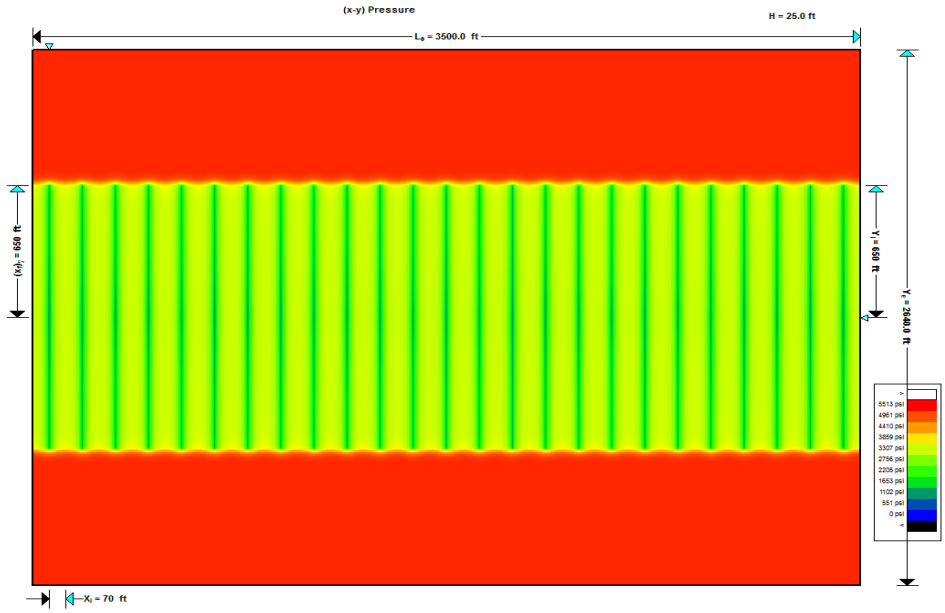

Figure 13. Pressure distribution in the reservoir after 12 months of production

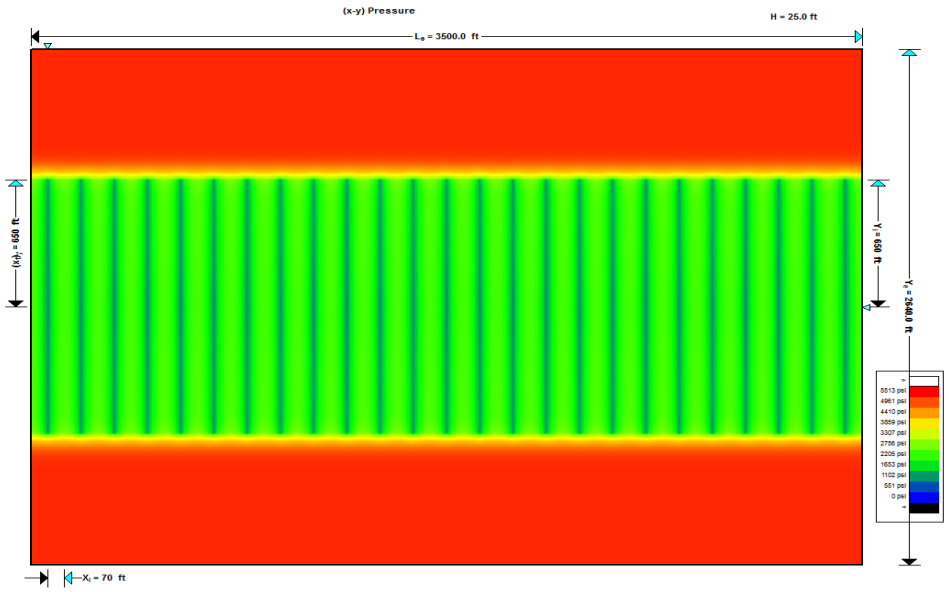

Figure 14. Pressure distribution in the reservoir after 84 months of production

The pressure distribution reaches uniformity in the SRV after 12 months of production and no production from the unstimulated region is observed. The flow from the unstimulated region begins after 84 months of production and the change in flow regime will be visible in RTA.

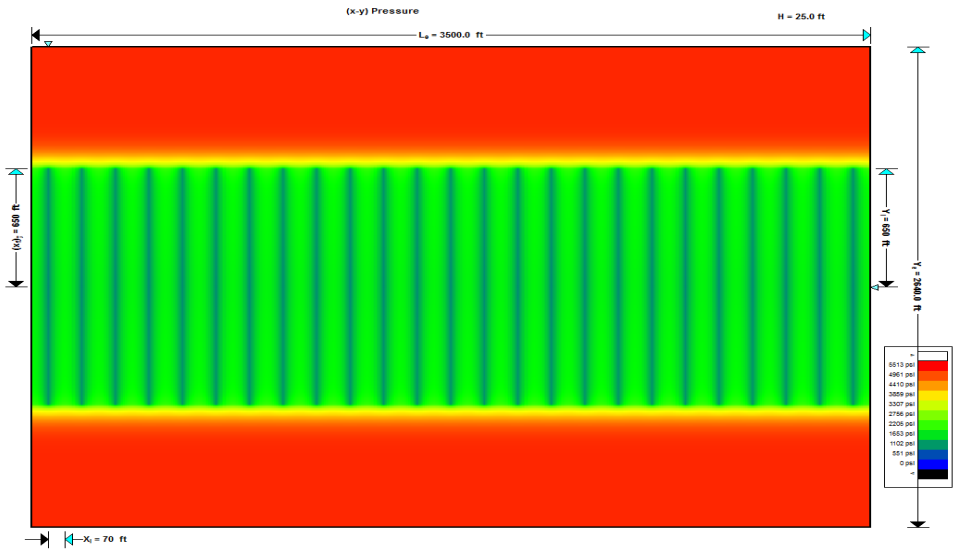

Figure 15. Pressure distribution in the reservoir after 134 months of production

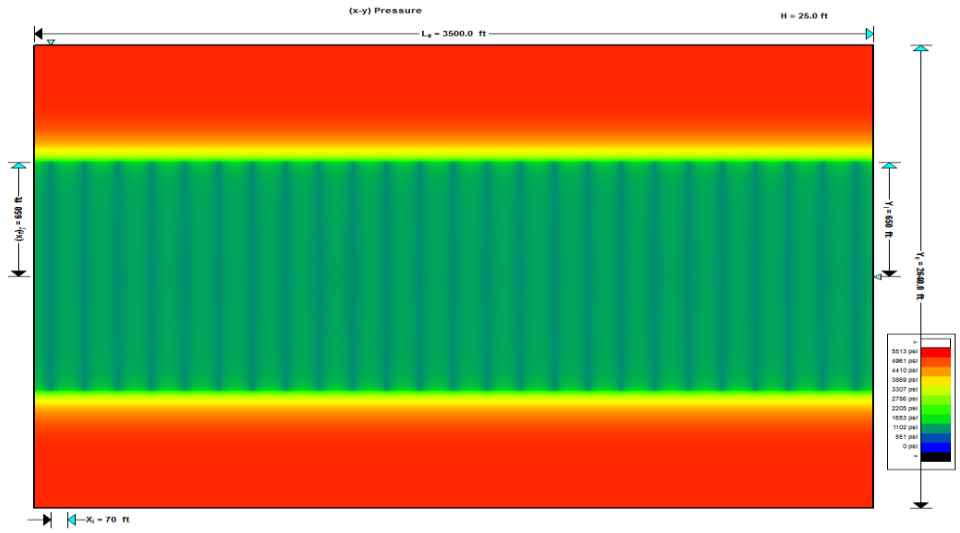

Figure 16. Pressure distribution in the reservoir after 300 months of production

The production from the unstimulated region is low as the pressure change has not probed significantly into this zone after 134 months of production. After 300 months of production, it is evident that only a small region of the unstimulated region is producing and that the SRV region has been significantly depleted. The following plots show the results of the

simulation. Figure 17 shows the production profile and Figure 18 shows the pressure decline in the reservoir.

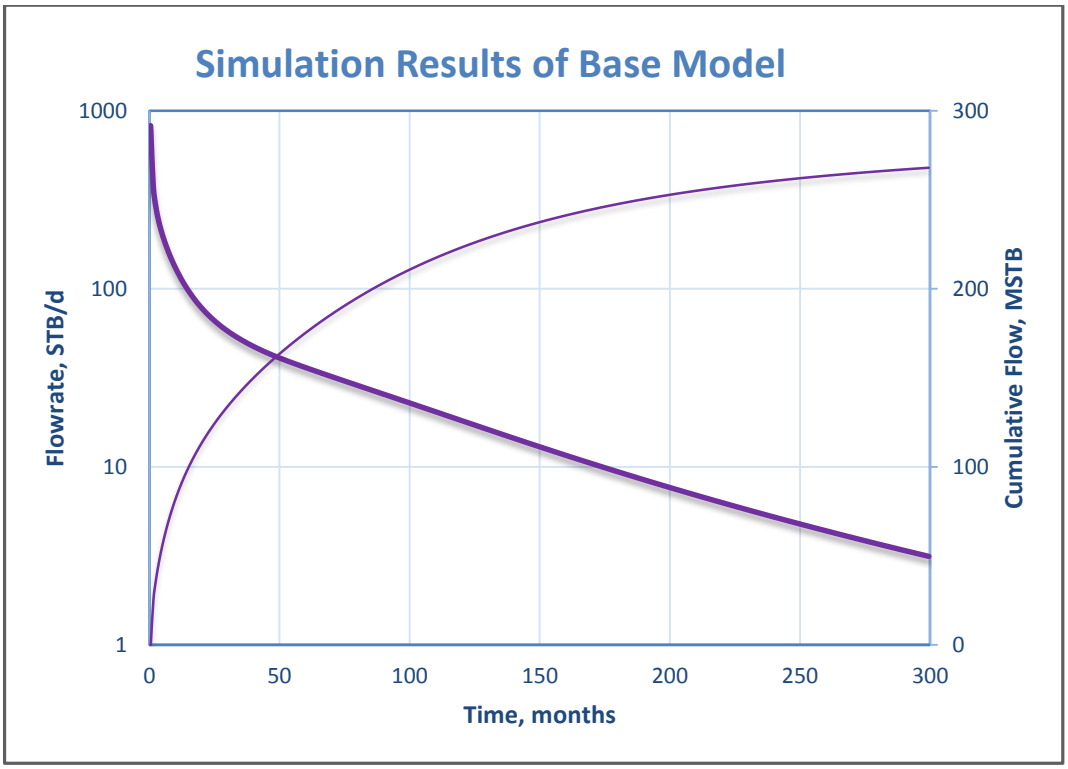

Figure 17. Simulation results of base model: production profile and cumulative production plots versus time in months

The diagnostic plots for the simulation are presented in the following figures. Figure 19 and Figure 20 show Material Balance Time plot and Square-root of time respectively. The time to BDF is about 84 months from the diagnostic plots and 96 months from the depth of investigation equations. The switch from SEPD to Arps model is done at 84 months as shown in figure. Table shows the SEPD and Arps parameters used in the

example. Figure 21 shows the production forecast using the composite model and Table 4 shows the decline curve parameters for each section.

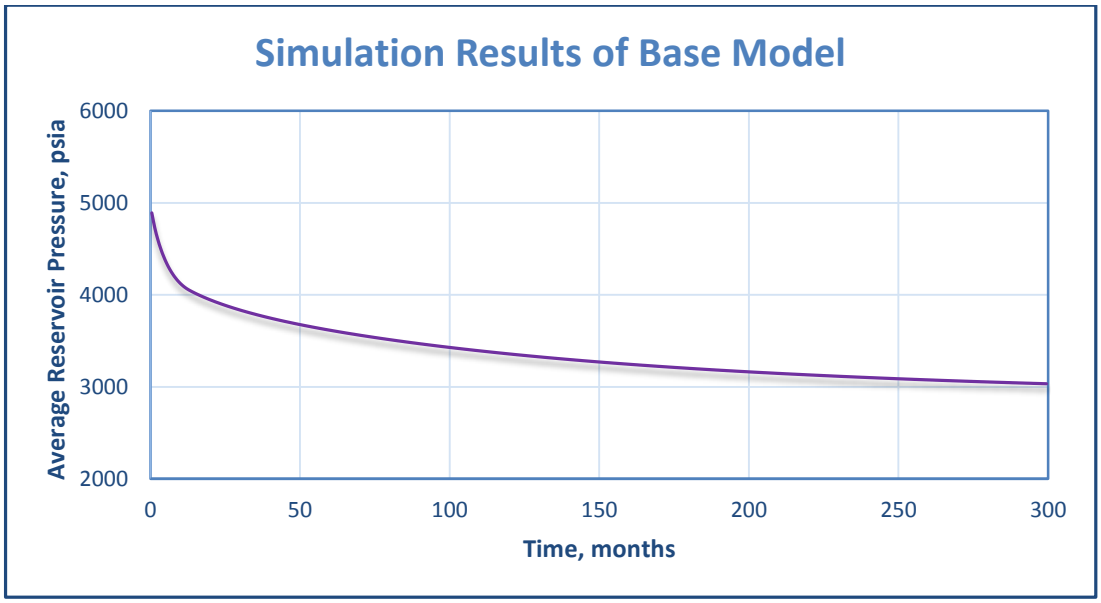

Figure 18. Simulation results of base model: average reservoir pressure decline with time

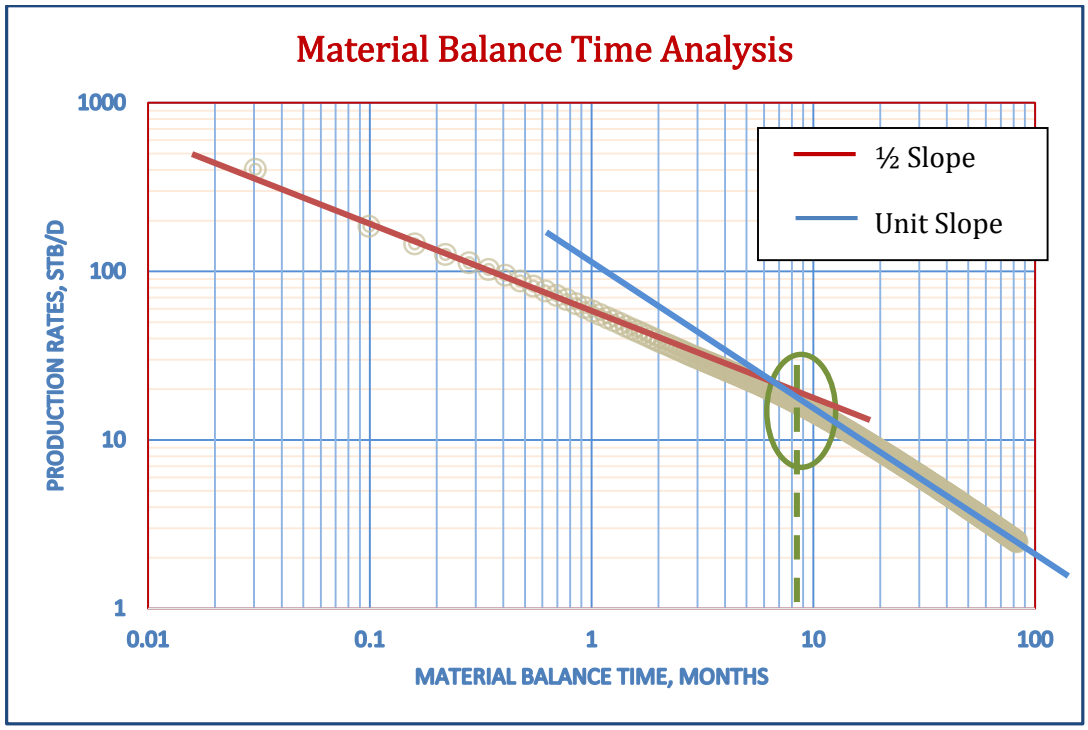

Figure 19. Material balance time analysis plot for the simulation results of base model

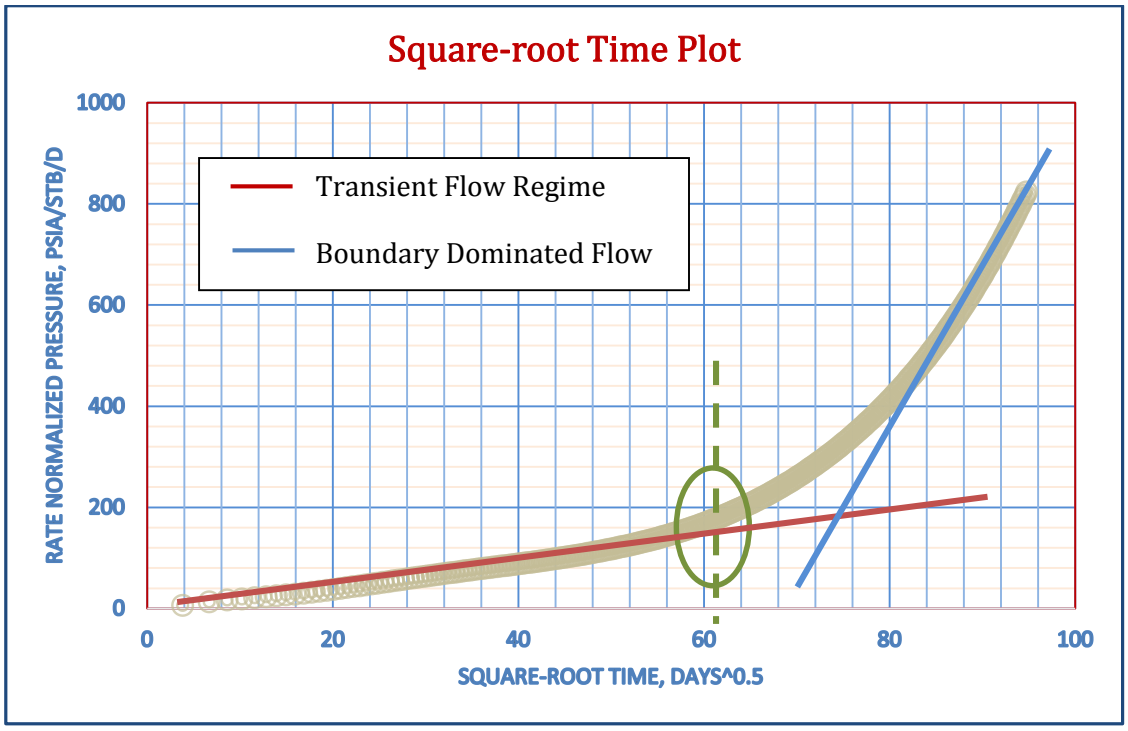

Figure 20. Square-root time analysis plot for the simulation results of base model

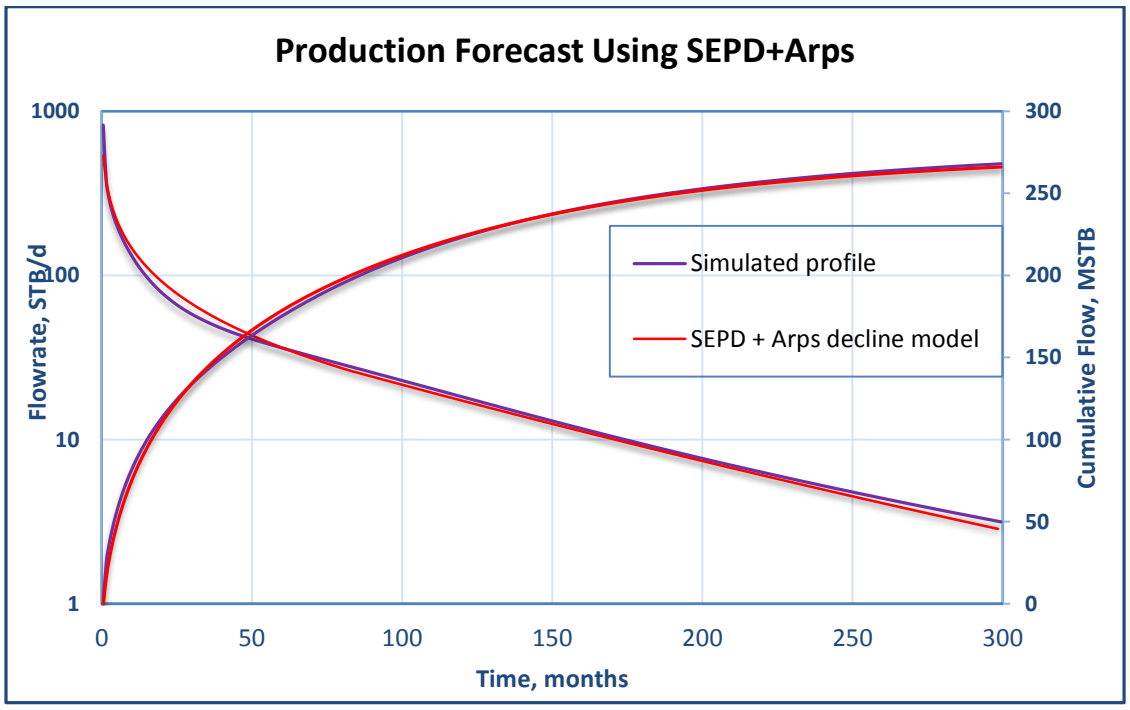

Figure 21. Production forecast using composite model for the base simulation results

Table 4. Decline model parameters for production forecast using the composite model

SEPD parameter		
η	q_i (STB/d)	τ (months)
0.25	1725	0.27
Switched from SEPD to Arps at 82.5 months		
Arps Parameters		
D_i (months^{-1})	q_i (STB/d)	b
0.012	71.5	0.1

We ran multiple simulations in which we changed the fracture completion parameters and reservoir permeability to develop a more complete understanding of sensitivity of EUR to these variables and sensitivity of Arps parameters to these parameters.

Chapter 5

Sensitivity Analysis of Parameters Affecting Production Performance

Recovery of reservoir fluids from shale resource plays depends on the fracture completion parameters and the Stimulated Reservoir Volume permeability generated by the fractures. The parameters discussed in this chapter are fracture half-length, fracture spacing, SRV permeability and matrix permeability.

5.1 Fracture Half-length

The fracture half-length is the most important parameter as the deeper the penetration into the reservoir, the larger the stimulated reservoir volume will be. In our study we chose a reservoir half-length of 1320 ft and we used fracture half-lengths of 300, 500, 650, 850 and 1000 ft to study the production performance. Figures 22 and 23 show the production profile and average reservoir pressure decline. As seen in the plots ultimate recovery is related directly to fracture half-length. Longer fractures yield better production. However, the characteristics of BDF vary with the penetration into the reservoir as depicted by Figure 24.

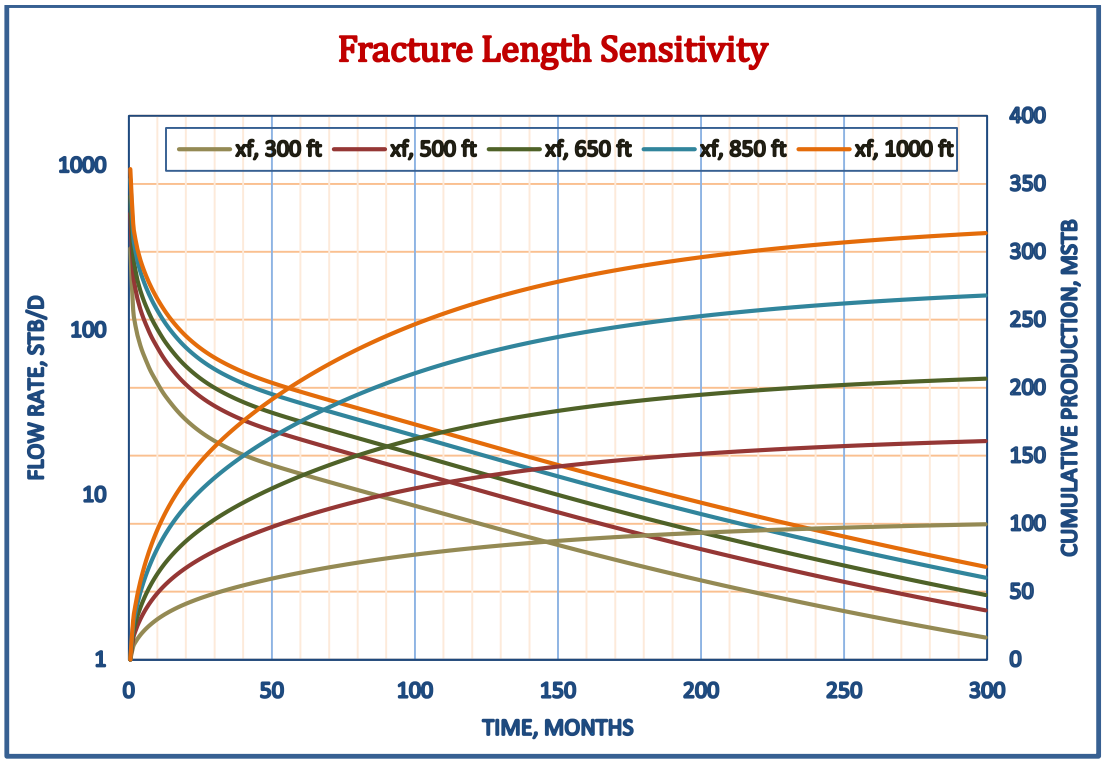

Figure 22. Fracture length sensitivity: production profile and cumulative production plots versus time in months.

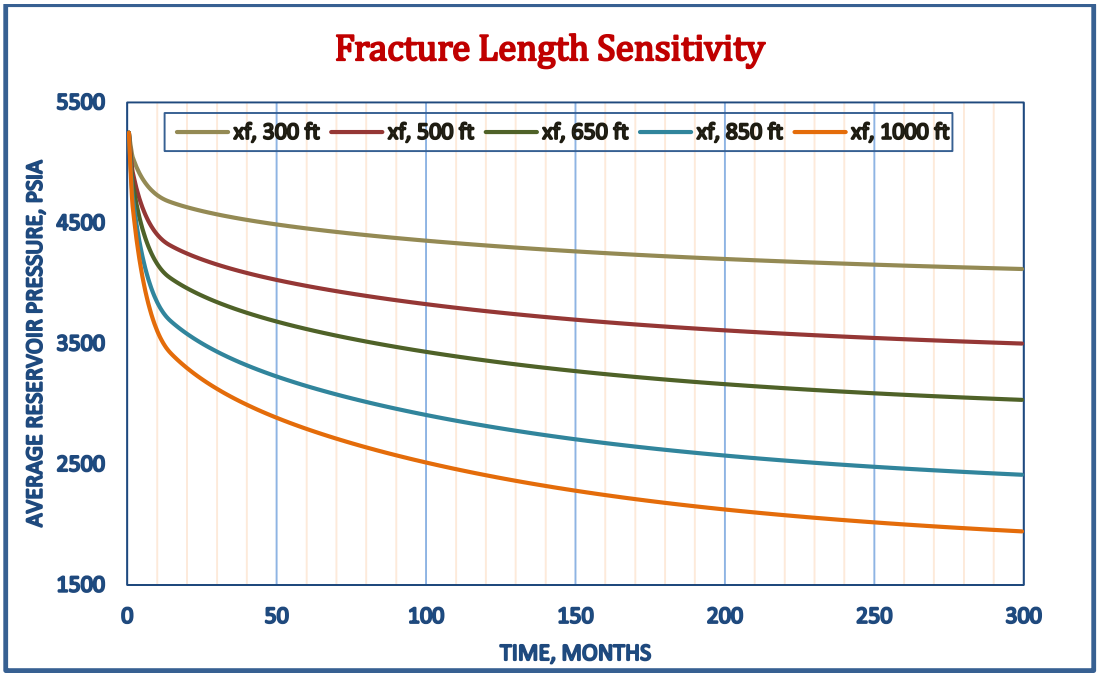

Figure 23. Fracture length sensitivity: average reservoir pressure decline with time.

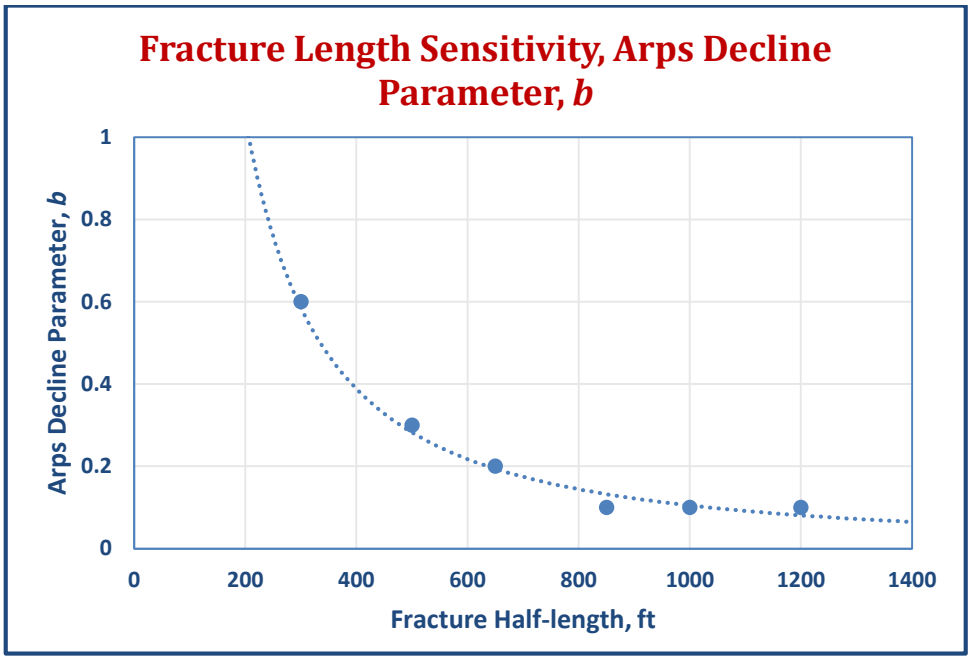

Figure 24. Fracture length sensitivity: Arps b parameter for the BDF regime.

At penetration ratios above 0.6 the behavior is noticed to be similar, with a b value of 0.1; the lower penetration ratios show an exponential increase in *b* values. All the b values came from matching the Fetkovich type curve and the b values are generated only to the nearest 0.1 at best.

5.2 Fracture Spacing

Designing the fracture spacing program is an important aspect for a completion engineer. It is difficult to determine the optimum spacing in the reservoir and it requires reservoir modeling and other financial considerations. In our study we have used spacing between the fractures

from 70 ft to 300 ft. The production profiles and pressure declines are shown in Figure 25 and Figure 26 respectively.

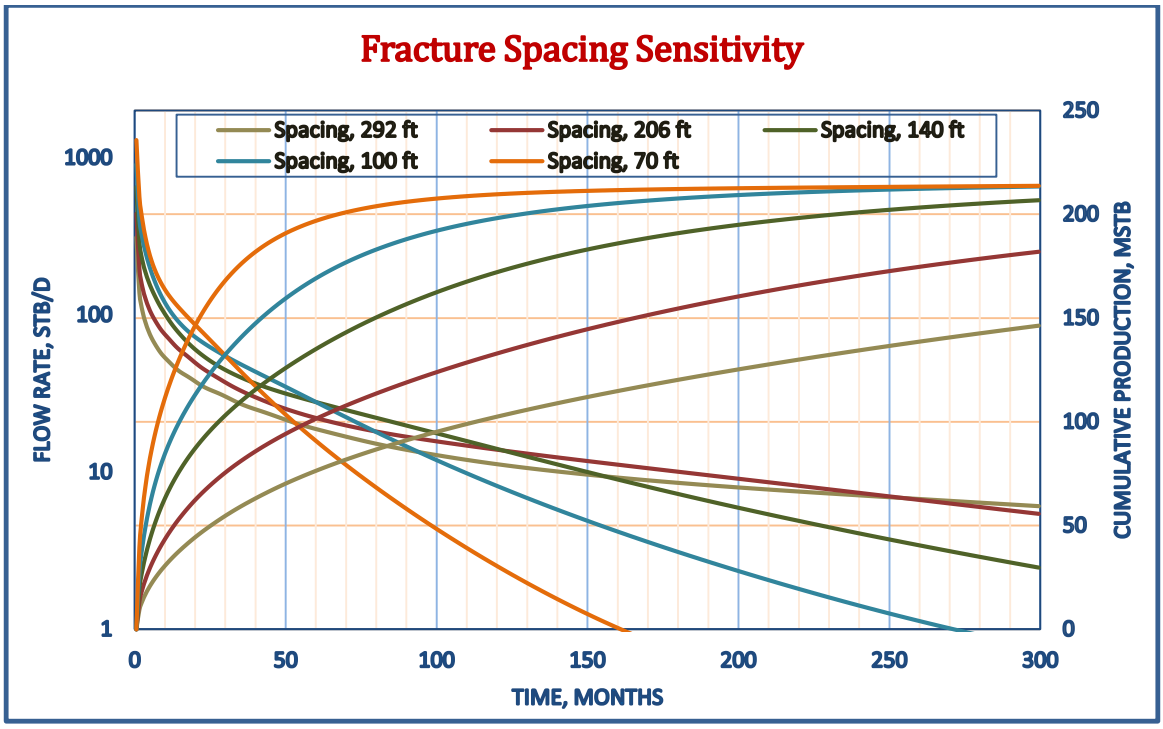

Figure 25. Fracture spacing sensitivity: production profile and cumulative production plots versus time in months.

The plots indicate that fracture spacing has a large impact on the ultimate recovery and the production profile. Closer spacing results in higher initial production but ultimately leads to about the same ultimate recovery. A better method for decision making would be to consider the net present value approach. Closer spacing requires more fracture stages and will have higher initial costs. Figure 28 shows the behavior of the Arps parameter b for the BDF. There are only two visible values because of the

graphical method used to estimate b (curve matching on the Fetkovic type curve) as shown in figures 27 and 29.

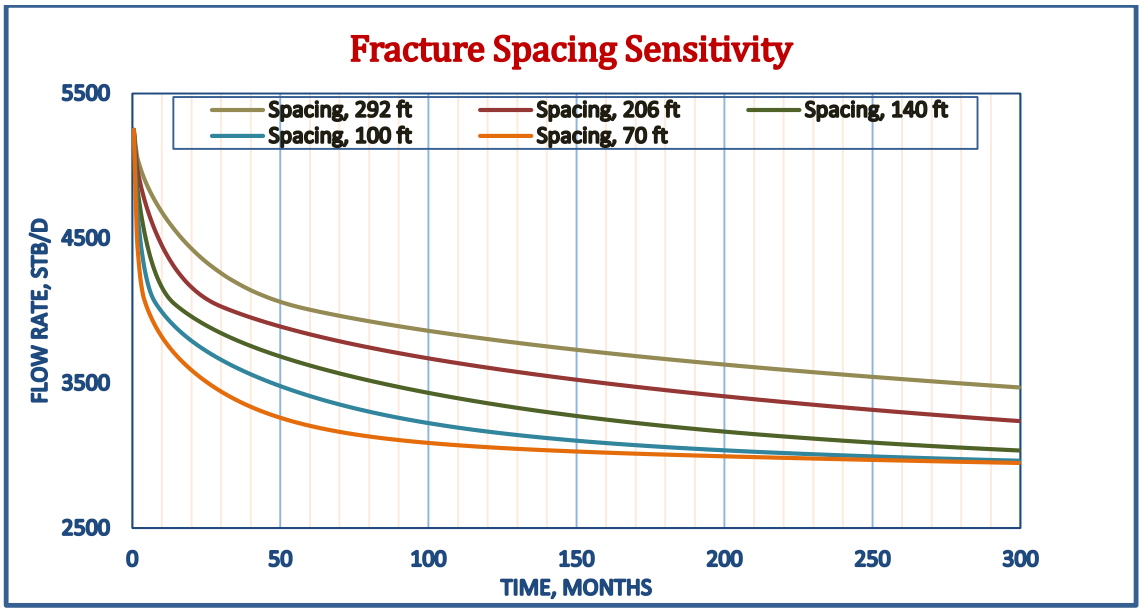

Figure 26. Fracture spacing sensitivity: average reservoir pressure decline with time.

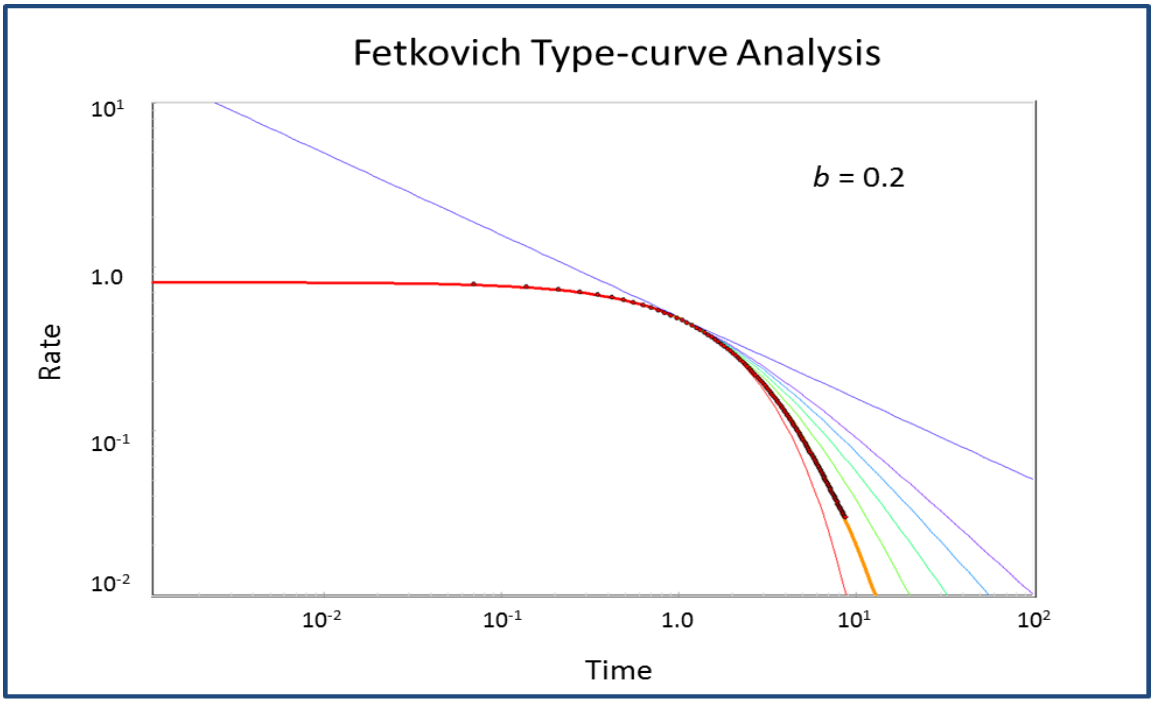

Figure 27. Fetkovich type curve analysis for simulated dataset.

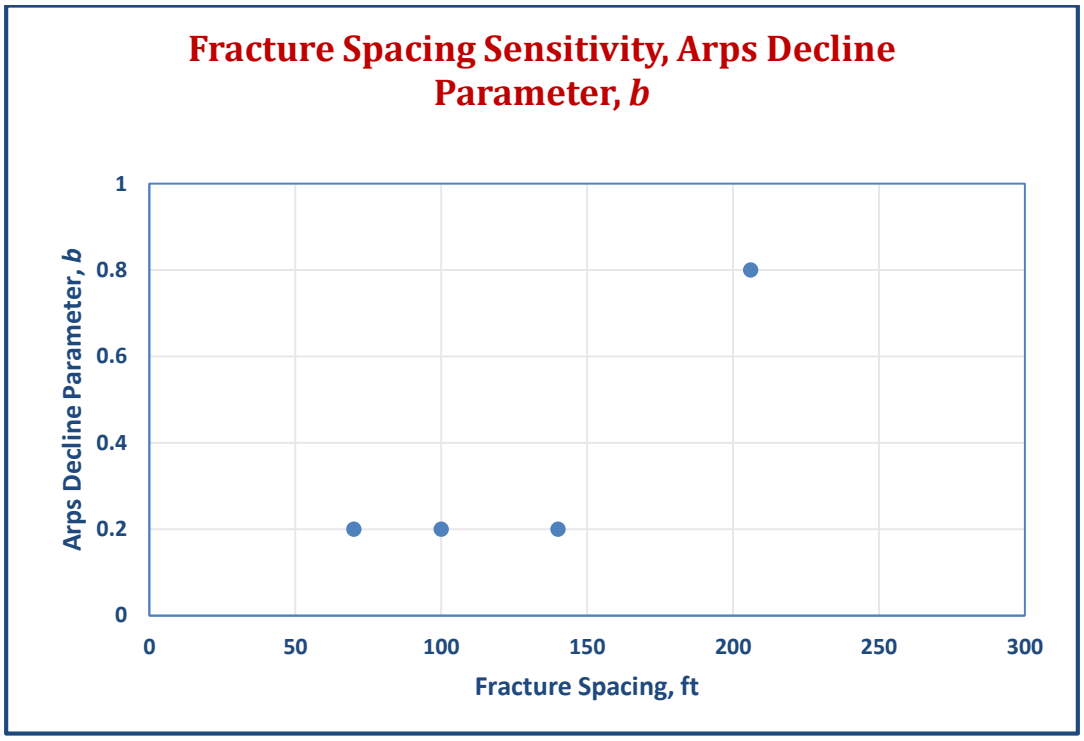

Figure 28. Fracture spacing sensitivity: Arps *b* parameter for the BDF regime.

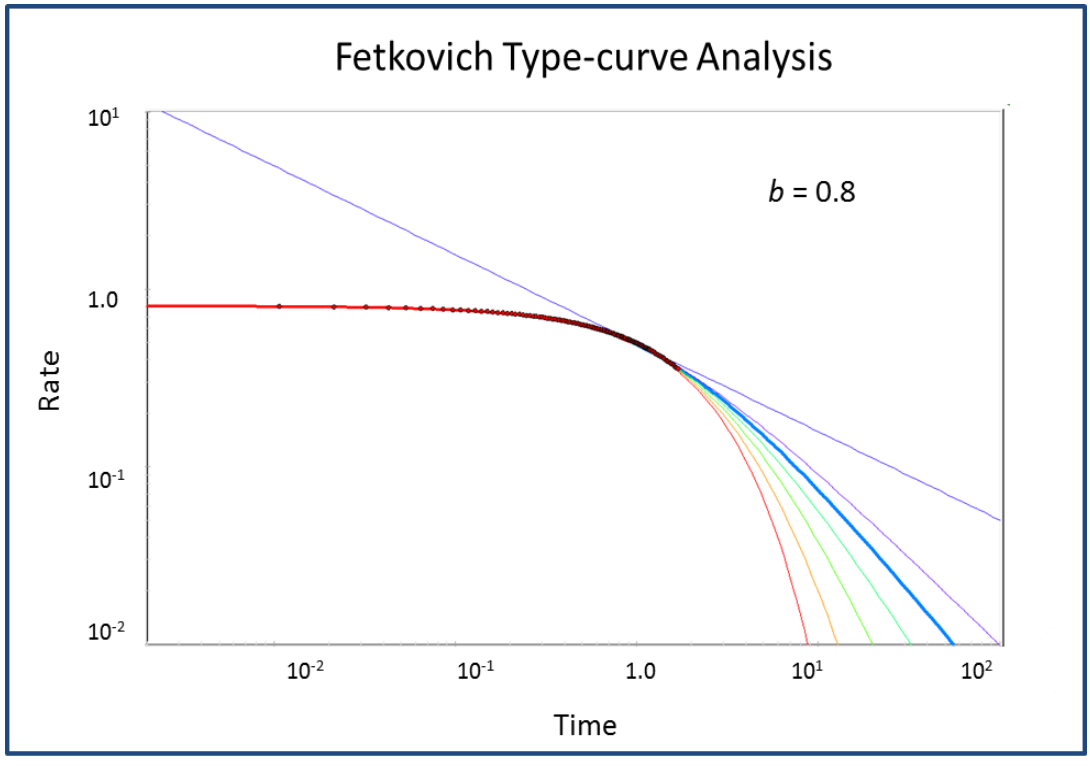

Figure 29. Fetkovich type curve analysis for simulated dataset.

5.3 SRV Permeability

We considered reservoirs with SRV permeability of 0.00001 mD, 0.0005 mD, 0.001 mD, 0.005 mD and 0.01 mD. The production profiles and average reservoir pressures of the simulation results are given in Figures 30 and 31. Change in permeability in this region can be attributed to the opening of closed natural fractures and change in stresses across the stimulated region.

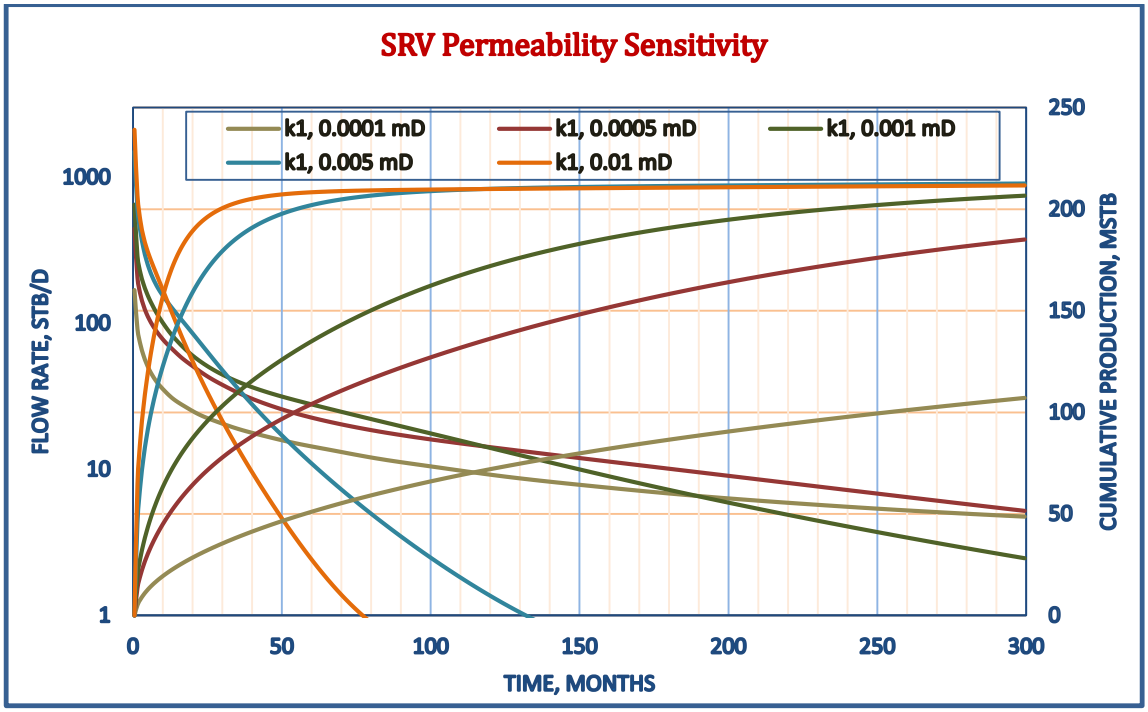

Figure 30. SRV permeability sensitivity: production profile and cumulative production plots versus time in months.

Figure 32 shows the Arps parameter b behavior. The *b* parameter tends to be in the range of 0.2 and 0.4 and the accuracy of this determination is limited by the accuracy of determining *b* graphically from a match on the Fetkovic type curve.

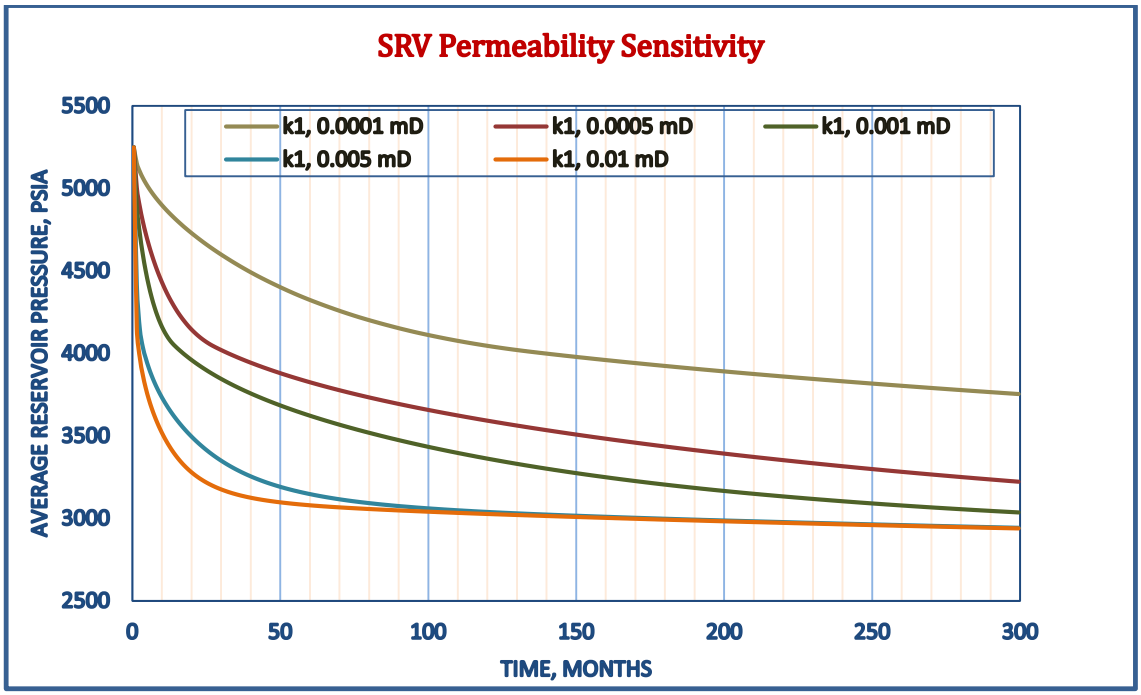

Figure 31. SRV permeability sensitivity: Average reservoir pressure plots versus time in months.

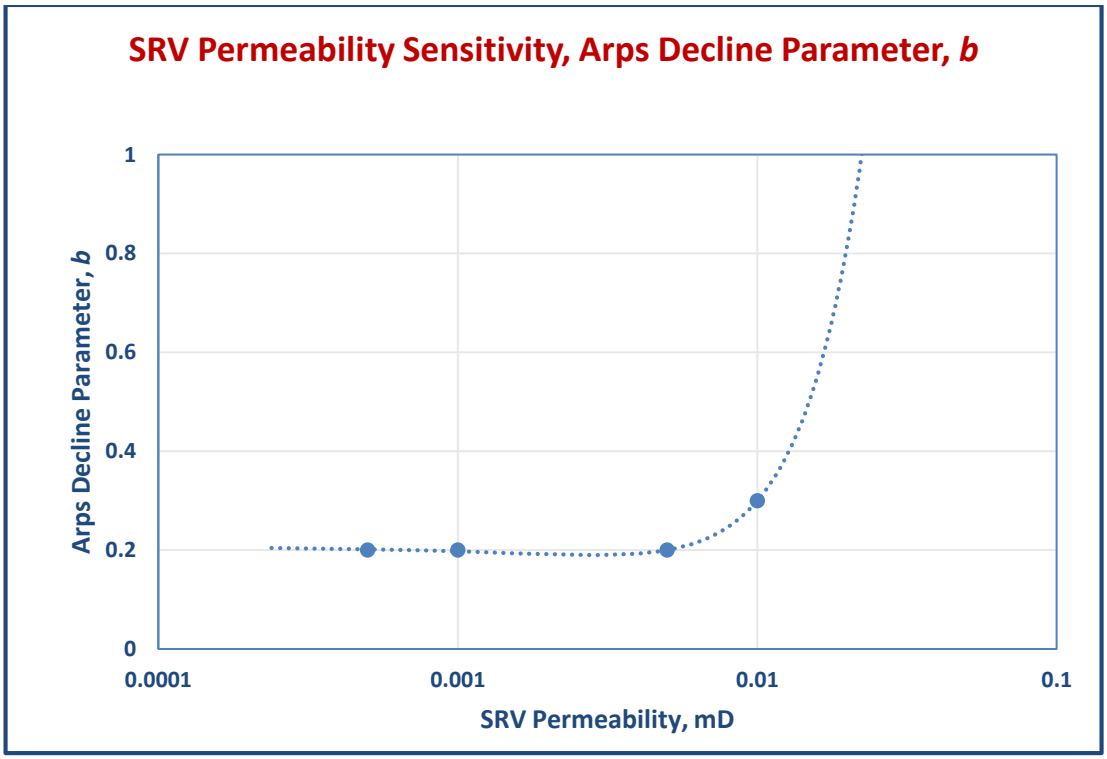

Figure 32. SRV permeability sensitivity: Arps *b* parameter for the BDF regime.

5.4 Unstimulated Matrix Permeability

As already discussed, the matrix permeability is very low in shale reservoirs. The unstimulated zone permeability is not expected to affect the production profile to a large extent. We used matrix permeability values of 0.00001 mD, 0.0001 mD, 0.0005 mD and 0.001 mD for our simulations. The production profiles and average reservoir pressures of the simulation results are given in Figure 33 and Figure 34. Despite the fact that the permeability in the unstimulated region has only a slight effect on recovery, it has a significant impact on the Arps b factor during BDF, as figure 35 shows.

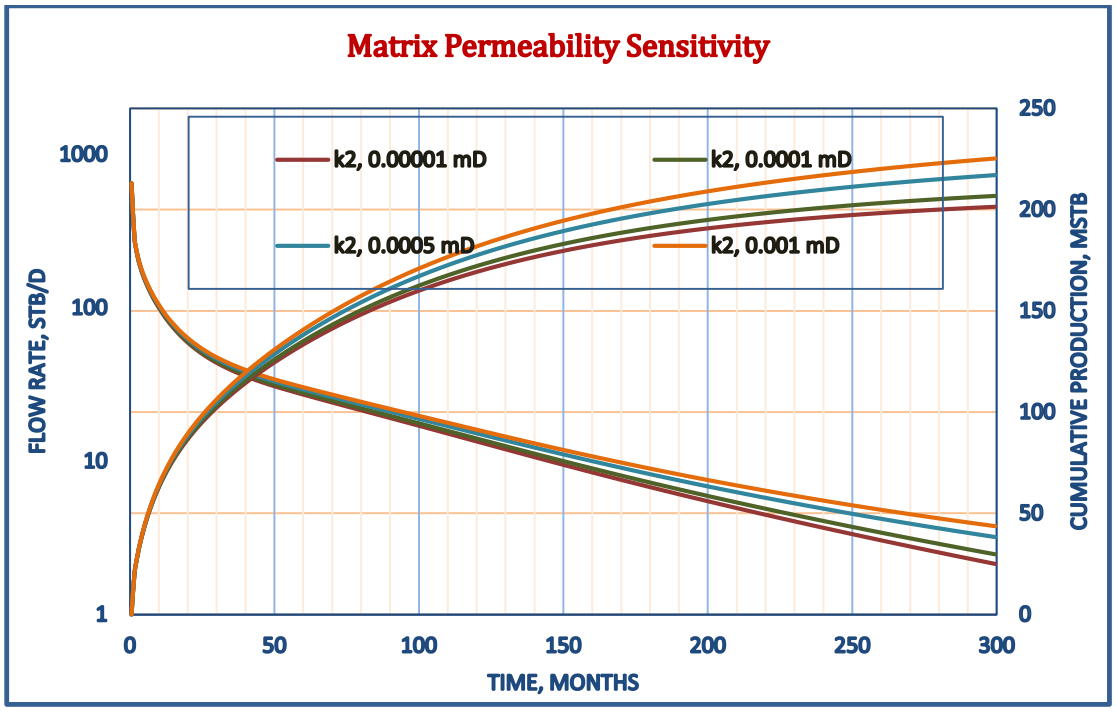

Figure 33. Unstimulated matrix permeability sensitivity: production profile and cumulative production plots versus time in months.

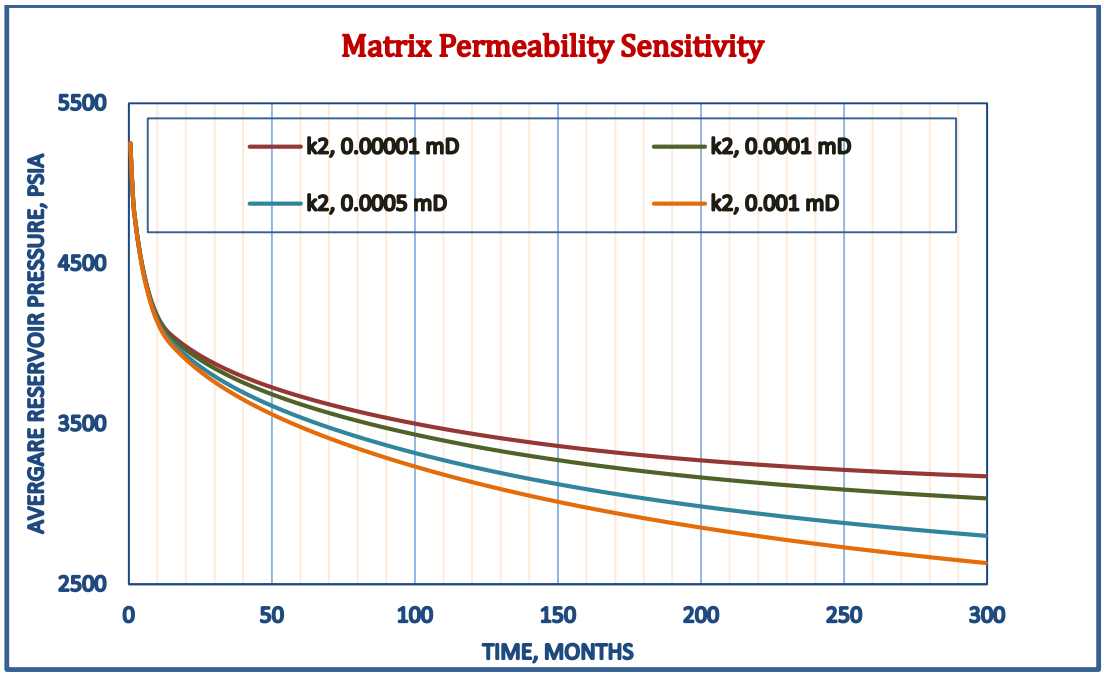

Figure 34. Unstimulated matrix permeability sensitivity: Average reservoir pressure plots versus time in months.

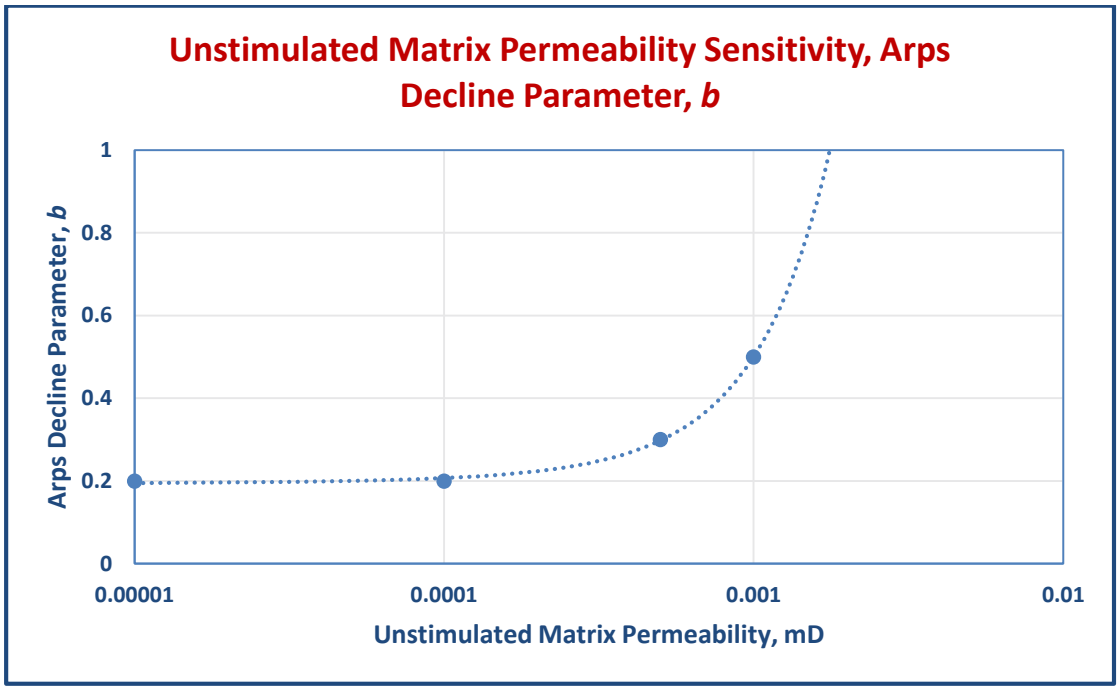

Figure 35. Unstimulated matrix permeability sensitivity: Arps *b* parameter for the BDF regime.

5.5 Comparative study of time to boundary dominated flow

As discussed in Chapter 3, the time to BDF can be calculated using depth of investigation equations and also estimating from the diagnostic plots. A comparative study of the results from these determinations is provided in Tables 5, 6, 7 and 8 and Figures 36, 37, 38 and 39.

Table 5. Comparative study of time to boundary dominated flow from depth of investigation equations and diagnostic plots for sensitivity to fracture half-length.

End of linear flow equations for sensitivity to fracture half-length		
Fracture Half-length (ft)	Time from diagnostic plot (months)	Time from depth of investigation equations (months)
300	180	97
500	97	97
650	84	97
850	83	97
1000	85	97
1200	71	97

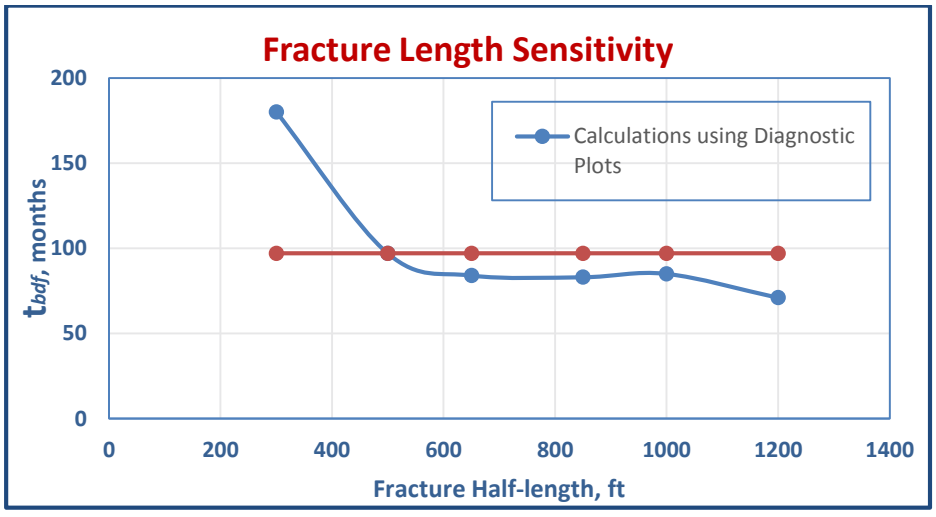

Figure 36. Fracture length sensitivity, time to BDF

Table 6. Comparative study of time to boundary dominated flow from depth of investigation equations and diagnostic plots for sensitivity to fracture spacing.

End of linear flow equations for sensitivity to fracture spacing		
Fracture Spacing (ft)	Time from diagnostic plot (months)	Time from depth of investigation equations (months)
70	74	51
100	93	97
140	84	97
206	150	210
292	370	415

Table 7. Comparative study of time to boundary dominated flow from depth of investigation equations and diagnostic plots for sensitivity to unstimulated matrix permeability.

End of linear flow equations for sensitivity to unstimulated matrix permeability		
Unstimulated matrix permeability (mD)	Time from diagnostic plot (months)	Time from depth of investigation equations (months)
0.00001	93	97
0.0001	84	97
0.0005	93	97
0.001	93	97

Table 8. Comparative study of time to boundary dominated flow from depth of investigation equations and diagnostic plots for sensitivity to SRV permeability.

End of linear flow equations for sensitivity to SRV permeability		
SRV permeability (mD)	Time from diagnostic plot (months)	Time from depth of investigation equations (months)
0.0001	930	970
0.0005	166	194
0.001	84	97
0.005	35	20

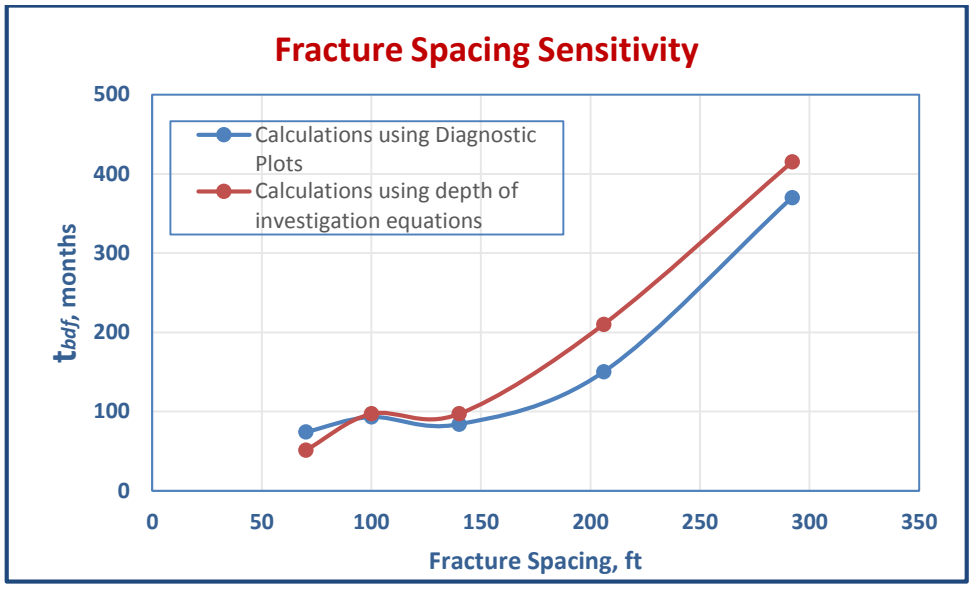

Figure 37. Fracture spacing sensitivity, time to BDF

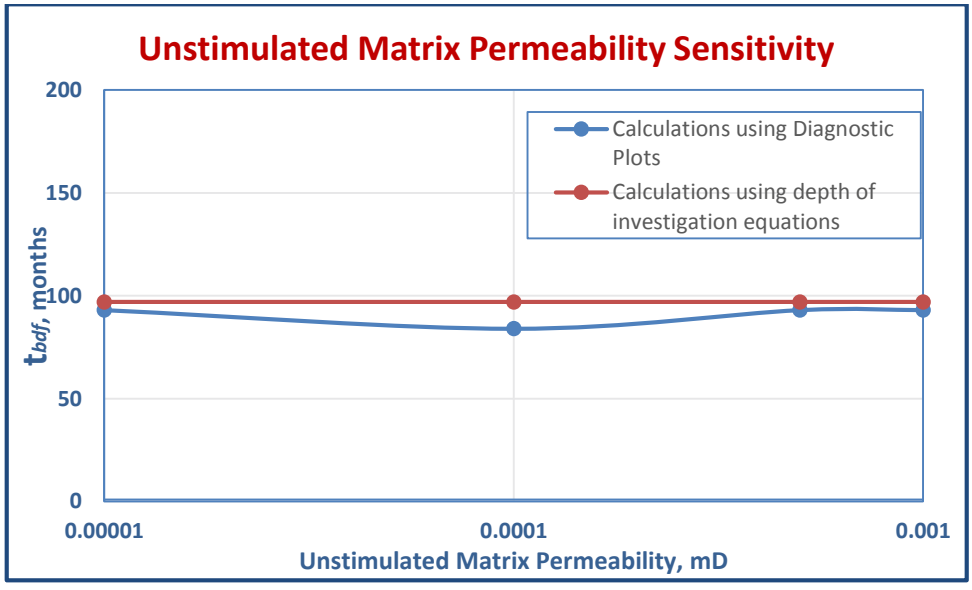

Figure 38. Unstimulated matrix permeability sensitivity, time to BDF

The results show that the depth of investigation equations comparable to those from when tested for sensitivity to fracture spacing, unstimulated matrix permeability and SRV permeability. However, when tested for

sensitivity to fracture half-length the results are not comparable to those estimated from the diagnostic plots. For shorter fractures, flow from beyond the ends of fractures is likely to be more important at earlier times, before fracture interference occurs.

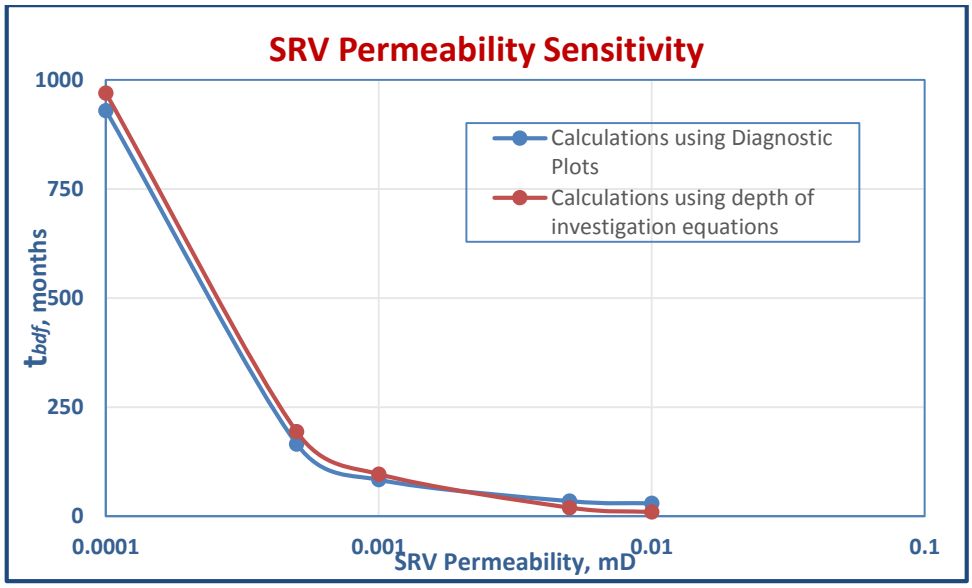

Figure 39. SRV permeability sensitivity, time to BDF

Chapter 6

Conclusions

Based on this study, the following conclusions can be drawn:

a. Appropriate decline models for production forecasting can be a combination of a linear flow model during transient flow, followed by a conventional Arps model during BDF.

b. Arps model with a b value in the range of 1.2 and 2.5 for all flow regimes is not reliable to provide the production forecast of shale liquids.

c. Time to BDF can be estimated reasonably accurately in advance using depth of investigation equations to determine time to fracture interference except in cases of short fractures accompanied by flow from the unstimulated matrix into the SRV.

d. The Arps decline parameter during BDF is influenced by hydraulic fracture spacing, fracture length, effective matrix permeability within the SRV, and unstimulated matrix permeability. Industrial use of switching to an Arps model with b value of zero during BDF provides inaccurate solutions.

In practice teams from reservoir engineering and production engineering departments should perform similar systematic studies on particular fields to determine the degree of change in Arps decline parameter. A detailed study would also provide the influence of the completion parameters on the production performance and the EUR.

A procedure for forecasting reserves using this study can be developed. For example, in situations with longer fractures and known fracture spacing, SRV permeability and unstimulated matrix permeability the time to BDF can be calculated using depth of investigation equations and based on the unstimulated matrix permeability sensitivity, a value for the Arps *b* parameter can be selected.

REFERENCES

Arps, J.J. 1945. *Analysis of Decline Curves.* Transactions of the AIME 160(1): 228-247. SPE 945228

Cox, S.A., Cook, D.M., Dunek, K., Daniels, R., Jump, C. and Barree, B., 2008. *Unconventional Resource Play Evaluation: A Look at the Bakken Shale Plays of North Dakota.* Paper SPE-114171 presented at the 2008 SPE Unconventional Reservoirs Conference held in Keystone, Colorado, 10-12 February 2008.

Fetkovich, M.J., 1980. *Decline Curve Analysis Using Type Curves.* SPE Journal of Petroleum Technology 32(6):1065-1077.

Kanfar, M.S., Alkouh, A.B. and Wattenbarger, R.A., 2013. *Modeling Guidelines for Analyzing and Forecasting Shale Well Performance.* Paper SPE-165698 presented at the SPE Eastern Regional Meeting held in Pittesburgh, Pennsylvania, 20-22 August 2013.

Kang, S.S., Datta-Gupta, A., and Lee, W.J. 2011. *Impact of Natural Fractures in Drainage Volume Calculations and Optimal Well Placement in Tight Gas Reservoirs.* Paper SPE 144338 presented at the North American Unconventional Gas Conference and Exhibition held in The Woodlands, Texas, USA, 14-16 June 2011.

Nobakht, M., Mattar, L., Moghadam S. and Anderson D.M. 2010. *Simplified yet Rigorous Forecasting of Tight/Shale Gas Production in Linear Flow.* Paper SPE 133615 presented at the SPE Western Regional Meeting held in Anaheim, California, USA, 27-29 May 2010.

Li, Q., Chen, M., Jin, Y., Zhou, Y., Wang, F.P. and Zhang, R., 2013. *Rock Mechanical Properties of Shale Gas Reservoir and Their Influences on Hydraulic Fracture.* Paper IPTC-16580 presented at the International Petroleum Technology Conference held in Beijing, China, 26-28 March 2013.

Lio, Y. and Lee, W.J., 1994. *Depth of Investigation for Hydraulic Fractured Wells: Field Applications.* Paper SPE-27664-MS presented at the SPE Permian Basin Oil and Gas Recovery Conference held in Midland, Texas, 16-19 March 1994.

Thompson, J.M., Viannet, O.M. and Anderson, D.M., 2011. *Advancements in Shale Gas Production Forecasting – A Marcellus Case Study.* Paper SPE-144436 presented at the SPE Americas Unconventional Gas Conference and Exhibition held in The Woodlands, TX, USA, 14-16 June 2011.

Tran, T., Sinurat, P. and Wattenbarger, R.A., 2011. *Production Characteristics of the Bakken Shale Oil.* Paper SPE-145684 presented at the SPE

Annual Technical Conference and Exhibition held in Denver, Colorado, USA, 30 October-2 November 2011.

Valko, P.P. and Lee, W.J., 2010. *A Better Way to Forecast Production from Unconventional Gas Wells.* Paper SPE-134231-MS presented at the SPE Annual Technical Conference and Exhibition held in Florence, Italy, 19-22 September 2010.

Xie, J., Gupta, N., King, M.J. and Datta-Gupta, A., 2012. *Depth of Investigation and Depletion Behaviour in Unconventional Reservoirs Using Fast Marching Methods.* Paper SPE-154532 presented at EAGE Annual Conference held in Copendagen, Denmark, 4-7 June 2012.